



Search for top quark decays via Higgs-boson-mediated flavor-changing neutral currents in pp collisions at $\sqrt{s} = 8 \text{ TeV}$

The CMS Collaboration*

Abstract

A search is performed for Higgs-boson-mediated flavor-changing neutral currents in the decays of top quarks. The search is based on proton-proton collision data corresponding to an integrated luminosity of 19.7 fb^{-1} at a center-of-mass energy of 8 TeV collected with the CMS detector at the LHC. Events in which a top quark pair is produced with one top quark decaying into a charm or up quark and a Higgs boson (H), and the other top quark decaying into a bottom quark and a W boson are selected. The Higgs boson in these events is assumed to subsequently decay into either dibosons or difermions. No significant excess is observed above the expected standard model background, and an upper limit at the 95% confidence level is set on the branching fraction $\mathcal{B}(t \rightarrow Hc)$ of 0.40% and $\mathcal{B}(t \rightarrow Hu)$ of 0.55%, where the expected upper limits are 0.43% and 0.40%, respectively. These results correspond to upper limits on the square of the flavor-changing Higgs boson Yukawa couplings $|\lambda_{tc}^H|^2 < 6.9 \times 10^{-3}$ and $|\lambda_{tu}^H|^2 < 9.8 \times 10^{-3}$.

Published in the Journal of High Energy Physics as doi:10.1007/JHEP02(2017)079.

1 Introduction

With the discovery of the Higgs boson (H) [1–3] it is possible to probe new physics by measuring its coupling to other particles. Of particular interest is the flavor-changing neutral current (FCNC) decay of the top quark to the Higgs boson. The investigation of this process at the CERN LHC is motivated by the large $t\bar{t}$ production cross section and the variety of possible decay modes of the Higgs boson.

The next-to-next-to-leading-order $t\bar{t}$ production cross section at a center-of-mass energy of 8 TeV and with a top quark mass (m_t) of 173.5 GeV [4] is 252 pb [5]. The standard model (SM) predicts that the top quark decays with a branching fraction of nearly 100% into a bottom quark and a W boson ($t \rightarrow Wb$).

In the SM, FCNC decays are absent at leading-order and occur only via loop-level processes that are additionally suppressed by the Glashow-Iliopoulos-Maiani mechanism [6, 7]. Because the leading-order decay rate of $t \rightarrow Wb$ is also quite large, the SM branching fraction $\mathcal{B}(t \rightarrow Hq)$, where q is an up or charm quark, is predicted to be of $\mathcal{O}(10^{-15})$ [6–8], far below the experimental sensitivity at the LHC. However, some extensions of the SM predict an enhanced $t \rightarrow Hq$ decay rate. Thus, observation of a large branching fraction would be clear evidence for new physics. The largest enhancement in $\mathcal{B}(t \rightarrow Hq)$ is predicted in models that incorporate a two-Higgs doublet, where the branching fraction can be of $\mathcal{O}(10^{-3})$ [8].

Previous searches for FCNC in top quark decays mediated by a Higgs boson have been performed at the LHC by ATLAS [9, 10] and CMS [11]. The CMS search considered both multilepton and diphoton final states and the observed upper limit of $\mathcal{B}(t \rightarrow Hc)$ at the 95% confidence level (CL) was determined to be 0.56%. The recent ATLAS result included final states where the Higgs boson decays to b quark pairs, and measured the observed upper limits of $\mathcal{B}(t \rightarrow Hc)$ and $\mathcal{B}(t \rightarrow Hu)$ at the 95% CL to be 0.46% and 0.45%, respectively.

The analysis presented here uses a data sample recorded with the CMS detector and corresponding to an integrated luminosity of 19.7 fb^{-1} of pp collisions at $\sqrt{s} = 8 \text{ TeV}$. The data were recorded in 2012 with instantaneous luminosities of $5\text{--}8 \times 10^{33} \text{ cm}^{-2}\text{s}^{-1}$ and an average of 21 interactions per bunch crossing. The inelastic collisions that occur in addition to the hard-scattering process in the same beam crossing produce mainly low- p_T particles that form the so-called “pileup” background.

In this paper, the FCNC decays $t \rightarrow Hc$ and $t \rightarrow Hu$ are searched for through the processes $t\bar{t} \rightarrow Hc + Wb$ or $Hu + Wb$. Three independent analyses are performed and their results are then combined. The multilepton analysis considers events with two same-sign (SS) leptons or three charged leptons (electrons or muons). This channel is sensitive to the Higgs boson decaying into WW , ZZ , or $\tau\tau$ which have branching fractions of 21.5%, 2.6%, and 6.3%, respectively [12]. The diphoton analysis considers events with two photons, a bottom quark, and a W boson that decays either hadronically or leptonically. The two photons in this channel are used to reconstruct the Higgs boson which decays to diphotons with $\mathcal{B}(H \rightarrow \gamma\gamma) = 0.23\%$ [12]. Finally, events with at least four jets, three of which result from the hadronization of bottom quarks (b jets), and a leptonically decaying W boson are considered. The b jet + lepton channel takes advantage of the large Higgs boson branching fraction into $b\bar{b}$ pairs, $\mathcal{B}(H \rightarrow b\bar{b}) = 57\%$ [13]. A summary of the enumerated final states is shown in Table 1.

The CMS detector and trigger are described in Section 2, and the event selection and reconstruction in Section 3. Section 4 then discusses the Monte Carlo (MC) simulation samples. The signal selection and background estimations for each of the three analyses are given in Section 5, and the systematic uncertainties in Section 6. Finally, the individual and combined results from the

analyses are presented in Section 7.

Table 1: Summary of the requirements for the $pp \rightarrow t\bar{t} \rightarrow Hq + Wb$ channels used in this analysis.

Decay channels	Leptons	Photons	Jets	b jets	Category
$H \rightarrow WW, ZZ, \tau\tau$ & $W \rightarrow \ell\nu$	$eee, ee\mu, e\mu\mu, \mu\mu\mu$	—	≥ 2	—	trilepton
$H \rightarrow WW, ZZ, \tau\tau$ & $W \rightarrow \ell\nu$	$e^\pm e^\pm, e^\pm \mu^\pm, \mu^\pm \mu^\pm$	—	≥ 2	—	dilepton SS
$H \rightarrow \gamma\gamma$ & $W \rightarrow \ell\nu$	e^\pm, μ^\pm	≥ 2	≥ 2	$=1$	diphoton + lepton
$H \rightarrow \gamma\gamma$ & $W \rightarrow q_1 q_2$	—	≥ 2	≥ 4	$=1$	diphoton + hadron
$H \rightarrow b\bar{b}$ & $W \rightarrow \ell\nu$	e^\pm, μ^\pm	—	≥ 4	≥ 3	b jet + lepton

2 The CMS detector and trigger

A detailed description of the CMS detector, together with a definition of the coordinate system used and the relevant kinematic variables, can be found in Ref. [14]. The central feature of the CMS apparatus is a superconducting solenoid, 13 m in length and 6 m in diameter, which provides an axial magnetic field of 3.8 T. Within the field volume there are several particle detection systems. Charged particle trajectories are measured by silicon pixel and strip trackers, covering $0 \leq \phi \leq 2\pi$ in azimuth and $|\eta| < 2.5$ in pseudorapidity. A lead tungstate crystal electromagnetic calorimeter (ECAL) surrounds the tracking volume. It is comprised of a barrel region $|\eta| < 1.48$ and two endcaps that extend up to $|\eta| = 3$. A brass and scintillator hadron calorimeter (HCAL) surrounds the ECAL and also covers the region $|\eta| < 3$. The forward hadron calorimeter (HF) uses steel as the absorber and quartz fibers as the sensitive material. The HF extends the calorimeter coverage to the range $3.0 < |\eta| < 5.2$. A lead and silicon-strip preshower detector is located in front of the ECAL endcaps. Muons are identified and measured in gas-ionization detectors embedded in the steel flux-return yoke outside the solenoid. The detector is nearly hermetic, allowing momentum balance measurements in the plane transverse to the beam direction.

Depending on the final state under consideration, events are selected at the trigger level by either requiring at least two leptons, (ee , $\mu\mu$ or $e\mu$), at least two photons, or a single lepton (e or μ) to be within the detector acceptance and to pass loose identification and kinematic requirements.

The dilepton triggers used in the multilepton selection require one lepton with $p_T > 17$ GeV and one lepton with $p_T > 8$ GeV. At the trigger level and during the offline selection, electrons are required to be within $|\eta| < 2.5$, and muons are required to be within $|\eta| < 2.4$. All leptons must be isolated, as described in Section 3, and have $p_T > 20$ GeV for the highest- p_T lepton, and $p_T > 10$ GeV for all subsequent leptons in the event. For events satisfying the full multilepton selection, the dimuon, dielectron, and electron-muon trigger efficiencies are measured to be 98%, 91%, and 94%, respectively, for the SS dilepton selection, and 100% for the tripleton selection.

The diphoton trigger requires the presence of one photon with $p_T > 36$ GeV and a second photon with $p_T > 22$ GeV. Loose isolation and shower shape requirements are applied to both photons [15]. The average diphoton trigger efficiency is measured to be 99.4% after applying the full event selection for photons within $|\eta| < 2.5$, excluding the barrel-endcap transition region $1.44 < |\eta| < 1.57$.

The b jet + lepton selection uses the single-lepton triggers. The single-muon trigger requires at

least one isolated muon with $p_T > 24 \text{ GeV}$ and $|\eta| < 2.1$ to be reconstructed online. The single-electron trigger requires at least one isolated electron with $p_T > 27 \text{ GeV}$ and $|\eta| < 2.5$. The offline selection further requires that electrons have $p_T > 30 \text{ GeV}$ and muons have $p_T > 26 \text{ GeV}$. This results in an average trigger efficiency of 84% for the single-electron triggers and 92% for the single-muon trigger after the b jet + lepton selection.

3 Event selection and reconstruction

Events are required to have a primary vertex with a reconstructed longitudinal position within 24 cm of the geometric center of the detector and a transverse position within 2 cm from the nominal interaction point. To distinguish the hard-scattering vertex from vertices arising from pileup interactions, the reconstructed vertex with the highest scalar sum of the p_T^2 of its associated tracks is chosen as the primary vertex. To ensure that leptons originate from the same primary vertex, a loose requirement is applied to their longitudinal and transverse impact parameters with respect to the primary vertex.

The particle-flow event algorithm [16, 17] is used to reconstruct and identify individual particles using an optimized combination of information from the elements of the detector. Prompt electrons and muons arising from W and Z decays are typically more isolated than nonprompt leptons arising from the decay of hadrons within jets. In order to distinguish between prompt and nonprompt lepton candidates, a relative isolation parameter is defined for each lepton candidate. This is calculated by summing the p_T of all charged and neutral particles reconstructed using the particle-flow algorithm within a cone of angular radius $\Delta R \equiv \sqrt{(\Delta\eta)^2 + (\Delta\phi)^2} = 0.4$ around the lepton candidate momentum, where $\Delta\eta$ and $\Delta\phi$ are the pseudorapidity and azimuthal angle (in radians) differences, respectively, between the directions of the lepton and the other particle [18, 19]. This cone excludes the lepton candidate and the charged particles associated with the pileup vertices. The resulting quantity is corrected for additional underlying-event activity owing to neutral particles [3], and then divided by the lepton candidate's p_T . The relative isolation parameter is required to be less than 0.15 for electrons and 0.12 for muons.

The electron selection criteria are optimized using a multivariate approach that combined information from both the tracks and ECAL clusters, and have a combined identification and isolation efficiency of approximately 60% at low p_T (10 GeV) and 90% at high p_T (50 GeV) for electrons from W or Z boson decays [20]. The training of the multivariate electron reconstruction is performed using simulated events, while the performance is validated using data.

Muon candidates are reconstructed with a global trajectory fit using hits in the tracker and the muon system. The efficiency for muons to pass both the identification and isolation criteria is measured from data to be larger than 95% [3, 21].

For events in which there is an overlap between a muon and an electron, i.e., an electron within $\Delta R < 0.1$ of a muon, precedence is given to the muon by vetoing the electron. In the multi-lepton selection, events in which there are more than three isolated leptons (electron or muon) with $p_T > 10 \text{ GeV}$ are rejected to reduce diboson contamination. The invariant mass of dilepton pairs in the SS channel is required to be greater than 30 GeV in order to reject low-mass resonances and reduce poorly modeled backgrounds (e.g., QCD). In the b jet + lepton selection, events in which there are additional isolated electrons with $p_T > 20 \text{ GeV}$ and $|\eta| < 2.5$ or isolated muons with $p_T > 10 \text{ GeV}$ and $|\eta| < 2.4$ are rejected.

The photon energy is reconstructed from the sum of signals in the ECAL crystals [15]. The ECAL signals are calibrated [22], and a multivariate regression, developed for a previous $H \rightarrow$

$\gamma\gamma$ analysis [23], is used to estimate the energy of the photon. Clusters are formed from the neighboring ECAL crystals seeded around local maxima of energy deposits, and the collection of clusters that contain the energy of a photon or an electron is called a supercluster. Identification criteria are applied to distinguish photons from jets and electrons. The observables used in the photon identification criteria are the isolation variables, the ratio of the energy in the HCAL towers behind the supercluster to the electromagnetic energy in the supercluster, the transverse width in η of the electromagnetic shower, and the number of charged tracks matched to the supercluster. The photon efficiency identification is measured using $Z \rightarrow e^+e^-$ events in data by reconstructing the electron showers as photons [24], taking into account the shower shape and whether the electron probe is located in the barrel or endcap. The two highest p_T photons must exceed 33 and 25 GeV, respectively.

Jets are reconstructed from the candidates produced by the particle-flow algorithm. An anti- k_T clustering algorithm [25] with a distance parameter of 0.5 is used for jet reconstruction. Jets with a significant fraction of energy coming from pileup interactions or not associated with the primary vertex are rejected. Remaining pileup energy in jets is subtracted using a technique that relies on information about the jet area [26–28]. Reconstructed jets are calibrated to take into account differences in detector response [29]. The jets in the multilepton and b jet + lepton selections are required to have $p_T > 30$ GeV, $|\eta| < 2.5$, and to be separated from leptons such that $\Delta R(\text{lepton, jet}) > 0.3$. The selection of jets in the diphoton events differs by requiring the jet $E_T > 20$ GeV and the jets be separated from both photons such that $\Delta R(\text{photon, jet}) > 0.3$.

To characterize the amount of hadronic activity in an event, the scalar sum of the transverse energy of jets passing all of these requirements (H_T) is calculated. The missing transverse energy (E_T^{miss}) is calculated as the magnitude of the vector sum of the transverse momenta of all reconstructed particle-flow candidates in the event.

Jets originating from the hadronization of b quarks are identified by the combined secondary vertex (CSV) b tagging algorithm [30]. The selection criteria that are used have an identification efficiency of 66%, and a misidentification rate of 18% for charm quarks and 1% for light-quark and gluon jets. The diphoton and b jet + lepton selections require b-tagged jets. Although the identification of b jets is not used to select signal events in the multilepton selection, it is used for the purpose of defining control samples to check the normalization of simulated background processes. No additional tagging is used to discriminate between jets originating from c quarks.

The inclusion of b jets in the diphoton and b jet + lepton selections results in a difference in the sensitivity to the $t \rightarrow Hu$ and $t \rightarrow Hc$ decay modes. This is caused by the larger likelihood of b tagging a jet originating from a charm quark than from an up quark. The multilepton analyses do not include b tagging to enhance the signal sensitivity so the two FCNC top quark decay modes are indistinguishable.

4 Simulated samples

The determination of the expected signal and background yields relies on simulated events, as well as an estimation based on control samples in data, as discussed in later sections. Samples of Drell–Yan, $t\bar{t}$, W +jets, $W + b\bar{b}$, diboson, $t\bar{t} + Z$, $t\bar{t} + W$, and triboson events are generated using the MADGRAPH event generator (v5.1.5.11) [31]. The samples of ZZ to four charged leptons and single top quark events are generated using POWHEG (v1.0 r1380) [32–34]. In all cases, hadronization and showering are done through PYTHIA (v6.426) [35], and τ decays are simulated using TAUOLA (v2.75) [36]. Three additional production processes are considered

for the nonresonant diphoton backgrounds, where the dominant one coming from $\gamma\gamma + \text{jets}$ is simulated with SHERPA (v1.4.2) [37]. Top quark pairs with one additional photon are simulated with MADGRAPH, while those with two additional photons are simulated using the WHIZARD (v2.1.1) [38] generator interfaced with PYTHIA. The Z2 tune [39] of PYTHIA is used to model the underlying event.

Events that arise from the SM Higgs boson production are treated as a background. The gluon-fusion (ggH) and vector-boson-fusion (VBF) Higgs boson production processes are generated with POWHEG at next-to-leading order (NLO) in QCD, interfaced with PYTHIA. The associated W/ZH production and $t\bar{t}H$ processes are simulated with PYTHIA at leading order. The cross sections and branching fractions of the SM Higgs boson processes are set to the values recommended by the LHC Higgs cross section working group [12].

The simulated samples for the signal process $t\bar{t} \rightarrow Hq + Wb$ ($q = c$ or u) are produced using PYTHIA for the case of the Higgs boson decaying to $WW, ZZ, \tau\tau$, and $\gamma\gamma$, and with MADGRAPH for $H \rightarrow b\bar{b}$. The use of different generators is an artifact of the various modes being analyzed separately. The Higgs boson is assumed to have a mass of 125 GeV.

The set of parton distribution functions (PDF) used is CTEQ6L [40] in all cases, except for $H \rightarrow b\bar{b}$, where CT10 [41] is used.

The CMS detector response is simulated using a GEANT4-based (v9.4) [42] model, and the events are reconstructed and analyzed using the same software used to process collision data. The effect of pileup is included in the simulation process by superimposing simulated events on the process of interest. The simulated signal events are weighted to account for the differences between data and simulation of the trigger, reconstruction, and isolation efficiencies, and the distributions of the reconstructed vertices coming from pileup. Additional corrections are applied to account for the energy scale and lepton p_T resolution. The observed jet energy resolution and scale [29], top quark p_T distribution [43], and b tagging efficiency and discriminator distribution [44] in data are used to correct the simulated events. Corrections accounting for the differences in lepton selection efficiencies are derived using the tag-and-probe technique [45].

5 Signal selection and background estimation

The sensitivity of the search is enhanced by combining the twelve exclusive channels, shown in Table 1, defined according to the expected decay modes of the Higgs and W bosons.

5.1 Multilepton channels

The multilepton analysis is conducted with the goal of enhancing the signal sensitivity in the trilepton channel: $t\bar{t} \rightarrow Hq + Wb \rightarrow \ell\nu\ell\nu q + \ell\nu b$, and the SS dilepton channel: $t\bar{t} \rightarrow Hq + Wb \rightarrow \ell\nu qqq + \ell\nu b$, where ℓ represents either a muon or electron. The main target of optimization is final states resulting from $H \rightarrow WW$ decays.

In the case of the trilepton channel, rejection of events containing dileptons originating from resonant Z boson production is necessary to remove backgrounds from WZ production, asymmetric internal conversions (AIC, the process in which final-state radiation in a Drell–Yan event converts to dileptons where one of the leptons carries most of the photon momentum) [46] or final-state radiation where the photon is misidentified as an electron. A comparison of the two-dimensional distribution of the trilepton mass versus the opposite-sign dilepton mass is shown in Figure 1 for the estimated signal and background processes, and data. Events satisfying any of the following criteria are vetoed to reduce the contribution from resonant Z production: (1)

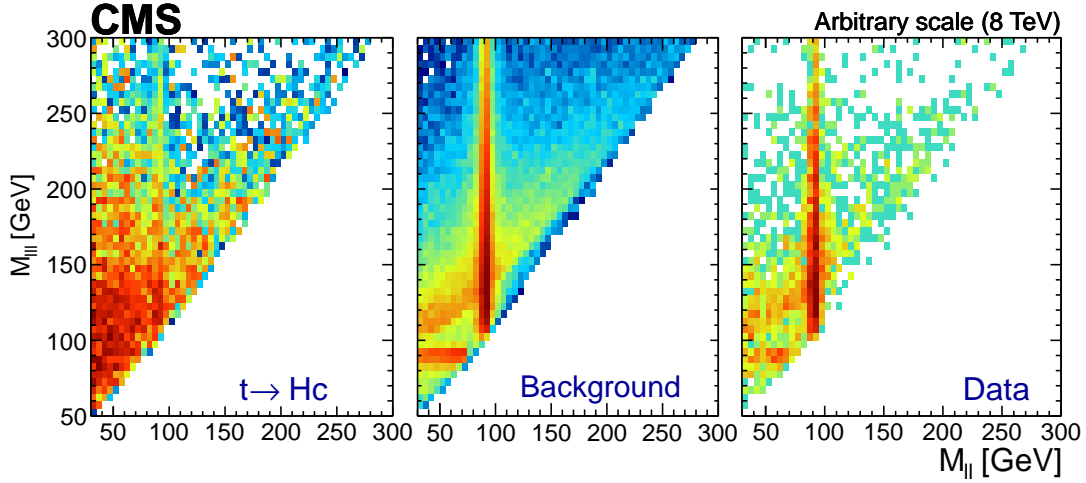


Figure 1: Trilepton invariant mass versus opposite-sign dilepton invariant mass in the trilepton channel after the event selection described in Section 3 for simulated signal, estimated background, and data, from left to right.

the invariant mass of an opposite-sign, same-flavor (OSSF) lepton pair is within 15 GeV of the Z boson mass [4]; (2) the invariant mass of an OSSF lepton pair is greater than 30 GeV and the trilepton invariant mass is within 10 GeV of the Z boson mass. For the SS dielectron channel, electron pairs with an invariant mass within 15 GeV of the Z boson mass are rejected to reduce the background arising from misidentification of the electron charge. No invariant mass requirement is applied to the $\mu^\pm\mu^\pm$ and $e^\pm\mu^\pm$ final states since there is a negligible contamination from resonant Z boson production.

The jet multiplicity after rejecting events containing a Z boson is shown in Figure 2. To improve the sensitivity of the search, we require at least two jets in the final state. Figure 3 shows the E_T^{miss} and H_T distributions for trilepton and SS dilepton events after applying the Z veto and jet requirement. A candidate event in the trilepton channel has no additional requirements on E_T^{miss} or H_T . The SS events are required to pass an E_T^{miss} -dependent H_T requirement (shown in Table 2) and have E_T^{miss} greater than 30 GeV. The E_T^{miss} and H_T requirements are obtained by maximizing the estimated signal significance, defined as the number of signal events over the square root of the number of background events.

The main sources of background can be divided into two categories according to the origin of the identified leptons and the E_T^{miss} . These include (1) *irreducible background processes*: events with leptons originating from the decay of SM bosons and having large E_T^{miss} arising from neutrinos; (2) *reducible background processes*: events with misidentified leptons produced either by nonprompt leptons from hadron decays (e.g., semileptonic decays of B mesons), by misidentified hadrons, or by mismeasurement of the lepton charge.

Given that at least two isolated leptons and two jets are required in the final state, the main sources of irreducible backgrounds are $t\bar{t}$ associated with vector boson production, $WZ \rightarrow 3\ell\nu$, $ZZ \rightarrow 4\ell$, $Z \rightarrow 4\ell$, and, to a lesser extent, triboson and $W^\pm W^\pm$ production. The contribution from all of these processes except $Z \rightarrow 4\ell$ production are estimated from simulated samples. The WZ cross section used in the simulation is cross-checked against a control sample from data that is enriched in WZ events by requiring that there be three leptons, with two of them

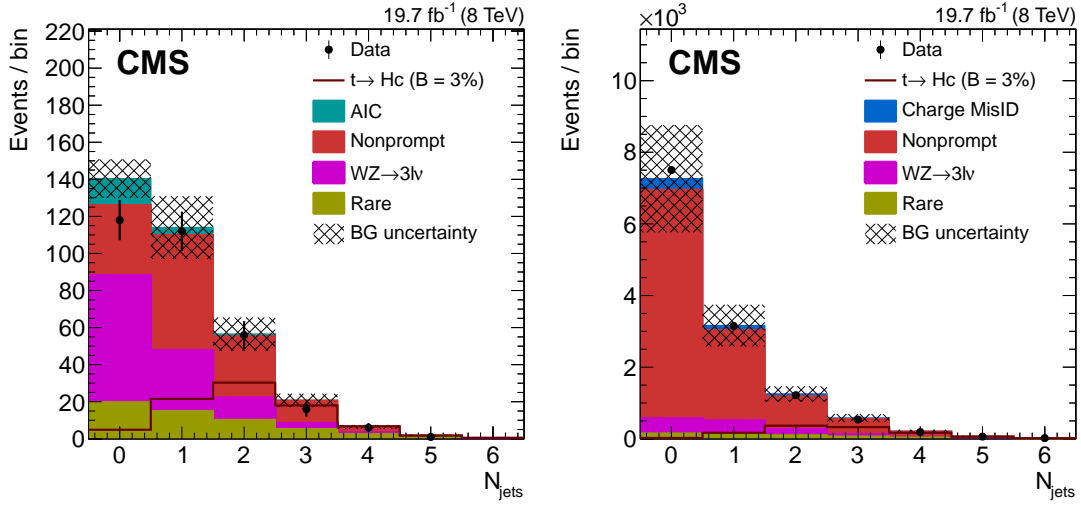


Figure 2: Jet multiplicity in the samples featuring three identified leptons (left) and two SS leptons (right) after rejecting events with Z bosons. The data are represented by the points with vertical bars, and the unfilled histogram shows the expected signal. A value of $\mathcal{B}(t \rightarrow Hc) = 3\%$ is used for the sake of improved visualization. The dominant backgrounds are represented with filled histograms and the background (BG) uncertainty is shown as shaded bands.

Table 2: Two-dimensional selection requirements on E_T^{miss} and H_T applied in the SS dilepton channel. An event is selected if it satisfies one of the three listed sets.

Selection set	1	2	3
E_T^{miss}	$<70 \text{ GeV}$	$70\text{--}90 \text{ GeV}$	$>90 \text{ GeV}$
H_T	$>140 \text{ GeV}$	$>100 \text{ GeV}$	$>60 \text{ GeV}$

forming a dilepton pair whose invariant mass is consistent with a Z boson. No correction to the WZ normalization is needed. This sample is also used to assess the systematic uncertainty in the simulation of the background.

For the presentation of the results, several of the backgrounds are grouped into a single category referred to as the rare backgrounds. The rare background contribution is estimated mainly from simulation (see the following paragraph), and the processes include $ZZ \rightarrow 4\ell$, $t\bar{t}+Z$, $t\bar{t}+W$, triboson, $W^\pm W^\pm$, and $t\bar{t}+H$. The $WZ \rightarrow 3\ell\nu$ background contribution is presented separately.

The residual contribution in the trilepton channel from asymmetric internal conversions (AIC) arising from Drell–Yan events is estimated using a data-driven technique [46] that uses $Z \rightarrow \ell^+\ell^- + \gamma$ events in data to model $Z \rightarrow \ell^+\ell^- + e/\mu$ events. This is because the process that gives rise to the two final states is the same (final-state radiation in Drell–Yan events), and the third lepton that is detected in the AIC event carries most of the photon momentum. The $\ell^+\ell^- + \gamma$ events are scaled based on photon p_T -dependent weights coming from a control sample defined as having a three-body invariant mass within 15 GeV of the Z boson mass. The average conversion probabilities for photons in dimuon and dielectron events are $(0.57 \pm 0.07)\%$ and $(0.7 \pm 0.1)\%$, respectively.

There are two major types of reducible backgrounds coming from $b\bar{b}$, Drell–Yan, W +jets, and $t\bar{t}$ processes. One source comes from events with either nonprompt leptons produced during the hadronization process of the outgoing quarks (e.g., semileptonic decays of B mesons) or

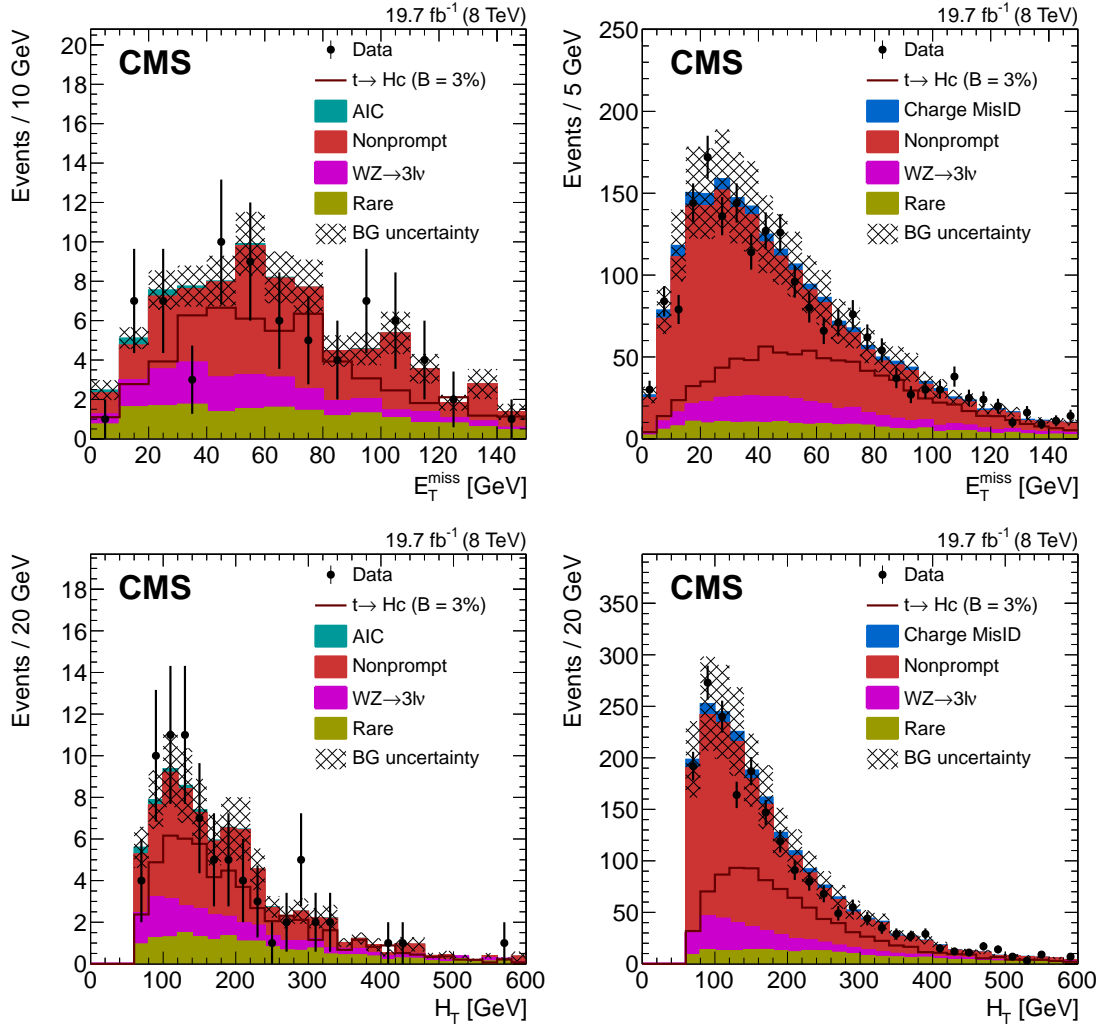


Figure 3: The E_T^{miss} (top) and H_T (bottom) distributions in the trilepton (left) and SS dilepton (right) channels in data (points with bars) and predicted by the SM background simulations (filled histograms) after rejecting events containing Z bosons, requiring at least two jets, and the event selection described in Section 3. The overall background uncertainty is shown in shaded black. The expected signal assuming a $\mathcal{B}(t \rightarrow Hc)$ of 3% is shown by the unfilled histogram.

hadrons misidentified as prompt leptons. The other source originates from the charge misidentification of a lepton in the more frequent production of opposite-sign dileptons. This background mostly contaminates the SS dielectron final states. Data-driven methods are used to estimate these two types of reducible backgrounds.

Mismeasuring the charge of a lepton can be a significant source of background in SS dilepton final states when there are one or more electrons. Even though the probability for mismeasuring the charge of an electron is relatively low ($\approx 0.1\%$), the production rate of opposite-sign dileptons is very high in comparison to processes that result in genuine SS dileptons. The probability of mismeasuring the charge of a muon is negligible ($< 10^{-6}$) and is therefore not considered here. In order to estimate the probability of misidentifying the charge of an electron from data, a control sample is selected consisting of events containing a dielectron pair with an invariant mass within 15 GeV of the Z boson mass. The rate of charge misidentification is then determined from the ratio of the number of SS events to opposite-sign events as a function of

Table 3: The predicted and observed inclusive event yields after the full event selection for the trilepton and SS dilepton categories assuming $\mathcal{B}(t \rightarrow Hq) = 1\%$. The quoted uncertainties include both statistical and systematic uncertainties added in quadrature. The total number of observed events is given in the last row.

Process	Trilepton		SS dilepton	
	Nonprompt	49.4 ± 9.0		409 ± 72
Charge misidentification	—		32.1 ± 6.4	
$WZ \rightarrow 3\ell\nu$	15.8 ± 1.1		83.9 ± 5.4	
Rare backgrounds	19.6 ± 1.4		128.1 ± 6.4	
Total background	86.2 ± 9.3		654 ± 73	
Signal	t→Hu	t→Hc	t→Hu	t→Hc
H→WW	12.4 ± 1.4	14.4 ± 1.1	135 ± 12	130.3 ± 8.1
H→ $\tau\tau$	4.1 ± 0.4	4.4 ± 0.3	36.4 ± 3.2	35.3 ± 2.2
H→ZZ	0.4 ± 0.1	0.4 ± 0.1	1.6 ± 0.1	1.4 ± 0.1
Total signal	16.9 ± 1.5	19.2 ± 1.1	173 ± 13	167.0 ± 8.4
Observed	79		631	

p_T and η . The measured charge misidentification for electrons with $|\eta| < 1.48$ is less than 0.2% for $p_T < 100$ GeV, while for $|\eta| > 1.48$ it is 0.1% at 10 GeV and increases with p_T to 2.5% at 125 GeV. These measurements are in agreement with those obtained from simulated Drell–Yan events.

Two control samples are used to estimate the misidentification rate of prompt leptons [47–49]: one region is enriched in $b\bar{b}$ events; the other is enriched in $Z + \text{jet}$ production. Both samples are used to estimate the probability of misidentifying nonprompt electrons and muons as a function of p_T and η . The measured misidentification rate for electrons ranges from 2% to 8% and for muons ranges from 1% to 6%. Simulated events are used to correct for the contamination arising from prompt leptons in the nonprompt misidentification rate measurement (e.g., WZ production in the $Z + \text{jet}$ control region). The rates are then applied to events where one or more of the lepton candidates fail the tight lepton identification requirements. The differences between the nonprompt misidentification rates in the two measurement regions and the signal region are then used to estimate the systematic uncertainty of this background. To further assess the systematic uncertainty, the misidentification rates are also measured in simulated events that reproduce the background composition of events in the signal region and compared to the rates measured from data.

The predicted numbers of background and signal events for the trilepton and SS dileptons are given in Table 3. The backgrounds are separated into nonprompt lepton, charge misidentification, $WZ \rightarrow 3\ell\nu$, and the rare backgrounds. The predicted number of signal events assumes $\mathcal{B}(t \rightarrow Hq) = 1\%$. The total number of observed events, also given in Table 3, is consistent with the predicted number of background events.

5.2 Diphoton channel

The diphoton analysis is performed using both leptonic and hadronic W boson decays: $t\bar{t} \rightarrow Hq + Wb \rightarrow \gamma\gamma q + \ell\nu b$, and $t\bar{t} \rightarrow Hq + Wb \rightarrow \gamma\gamma q + q\bar{q}b$. The mass of the diphoton system $m_{\gamma\gamma}$ is the primary variable used to search for the Higgs boson decay. The contribution of the nonresonant backgrounds is estimated by fitting the $m_{\gamma\gamma}$ distribution from data in the mass range $100 < m_{\gamma\gamma} < 180$ GeV, whereas the contribution of resonant backgrounds is taken from the simulation.

The two highest- p_T photons must have $p_T > m_{\gamma\gamma}/3$ and $p_T > m_{\gamma\gamma}/4$, respectively. The use of p_T thresholds scaled by $m_{\gamma\gamma}$ prevents a distortion of the low end of the $m_{\gamma\gamma}$ spectrum that would result from a fixed threshold [50]. In the rare case of multiple diphoton candidates in an event, the one with the highest p_T sum is selected.

The hadronic analysis uses events with at least four jets and exactly one b jet. The b jet and the three jets with the highest p_T are used to reconstruct the invariant mass of the two top quarks, $m_{j\gamma\gamma}$ and m_{bjj} . There are three possible $(m_{j\gamma\gamma}, m_{bjj})$ pairs per event. The combination of jets with the minimum value of $|m_{j\gamma\gamma}/m_{bjj} - 1| + |m_{bjj}/m_{j\gamma\gamma} - 1|$ is selected. The allowed ranges for $m_{j\gamma\gamma}$, m_{bjj} , and the W boson mass m_W associated with m_{bjj} are obtained by maximizing the signal significance S/\sqrt{B} in the simulation, where S is the number of signal events and B is number of the background events. The background events are assumed to come from $\gamma\gamma$ +jets and are taken from simulation. The highest signal significance is found to be 16% obtained for $142 \leq m_{bjj} \leq 222$ GeV, $158 \leq m_{j\gamma\gamma} \leq 202$ GeV, and $44 \leq m_W \leq 140$ GeV.

The leptonic analysis uses events with at least three jets, exactly one b jet, and at least one lepton. The reconstructed top mass $m_{b\ell\nu}$ is found from the b jet, the lepton, and E_T^{miss} . The longitudinal momentum of the neutrino is estimated by using the W boson mass as a constraint, which leads to a quadratic equation. If the equation has a complex solution, the real part of the solution is used. If the equation has two real solutions, the one with the smaller value of $|m_{j\gamma\gamma}/m_{b\ell\nu} - 1| + |m_{b\ell\nu}/m_{j\gamma\gamma} - 1|$ is chosen. The mass windows for m_{bjj} , $m_{j\gamma\gamma}$, and m_W are the same as in the hadronic channel.

The signal region is defined using the experimental width of the Higgs boson, 1.4 GeV, around the nominal mass peak position. As in the analysis of the inclusive SM Higgs boson decaying into diphotons [50], the signal shape of the diphoton invariant mass distribution is described by the sum of three Gaussian functions. Although the contribution from the SM Higgs boson background, dominated by the $t\bar{t}H$ process, is relatively small in comparison to the contribution of the nonresonant diphoton background, the resonant diphoton background cannot be ignored because it has a very similar $m_{\gamma\gamma}$ distribution as the signal.

To determine the shape of the nonresonant diphoton background, a function consisting of a test model and the resonant diphoton background is fitted to the data under the background-only hypothesis. The model of the resonant diphoton background is the same as the signal function. The background function is used to generate 1000 pseudo-experiment samples that are fitted with the background plus signal probability density function.

A pull is then defined as $(N_{\text{fit}} - N_{\text{gen}})/\sigma_{N_{\text{fit}}}$, where N_{fit} is the fitted number of signal events in the pseudo-experiments, N_{gen} is the number of generated signal events, and $\sigma_{N_{\text{fit}}}$ is the corresponding uncertainty. In the case under consideration, $N_{\text{gen}} = 0$. The procedure is verified by injecting signal in the pseudo-experiments. Several models are tried, and the chosen function for nonresonant diphoton background is the one whose bias (offset of the pull distribution) is less than 0.15 and with the minimum number of degrees of freedom for the entire set of tested models. A third-order Bernstein polynomial is selected as the functional form of the background for both the hadronic and leptonic channels. After determining the function to describe the nonresonant diphoton background, a function given by the sum of probability density functions of the resonant and nonresonant diphoton backgrounds and signal is fitted to the data. The normalization of the resonant diphoton background is allowed to vary within its uncertainties, while the normalization of the nonresonant component is unconstrained. Table 4 gives a summary of the observed and expected event yields for the two diphoton channels and Figure 4 shows the fit result overlaid with the data.

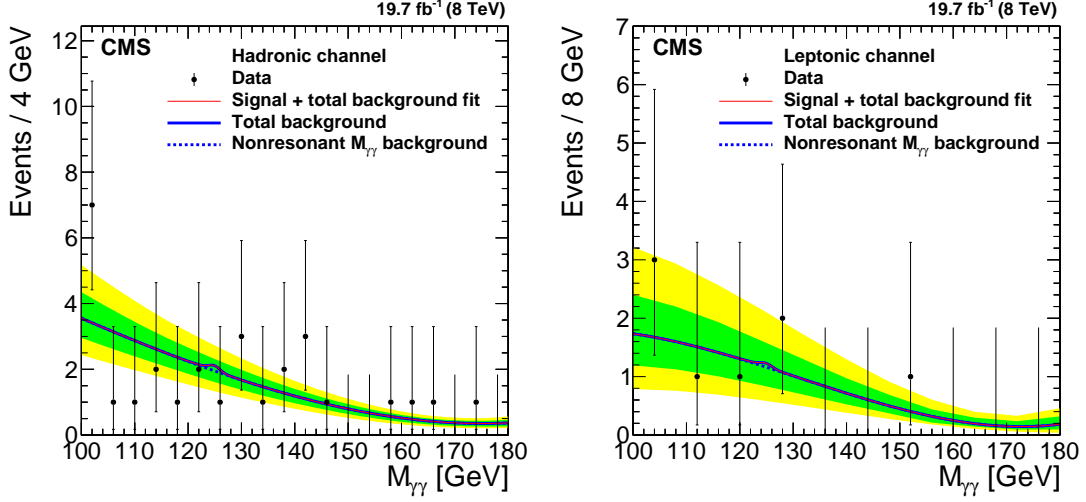


Figure 4: The $m_{\gamma\gamma}$ distribution and the fit result of the hadronic (left) and leptonic (right) channels. The dashed line represents the component of the nonresonant diphoton background, while the solid line represents the total background plus signal. The shaded bands represent one and two standard deviation uncertainties of the fit.

Table 4: Observed event yield and the expected numbers of background and signal events for the diphoton selection in the hadronic and leptonic channels in the $100 < m_{\gamma\gamma} < 180$ GeV mass range. The signal yields assume $\mathcal{B}(t \rightarrow Hq) = 1\%$. The uncertainties are statistical only.

Process	Hadronic channel	Leptonic channel
Nonresonant background	28.9 ± 5.4	8.0 ± 2.8
Resonant background	0.15 ± 0.02	0.04 ± 0.01
$t \rightarrow Hc$	6.26 ± 0.07	1.91 ± 0.04
$t \rightarrow Hu$	7.09 ± 0.08	2.02 ± 0.04
Observed	29	8

5.3 b jet + lepton channel

The basic event selection requirements for the b jet + lepton channel are a single-lepton trigger, one isolated lepton, a minimum E_T^{miss} of 30 GeV, and at least four jets, with at least three of them tagged as b jets. The background is dominated by $t\bar{t} \rightarrow b\bar{b}W^+W^-$ production. Figure 5 shows the distributions of E_T^{miss} and the W boson transverse mass (M_T) for data and simulation after the basic event selection criteria are applied. The transverse mass is defined as

$$M_T = \sqrt{2p_T^\ell E_T^{\text{miss}} [1 - \cos(\Delta\phi(\ell, \nu))]},$$

where p_T^ℓ is the p_T of the lepton, E_T^{miss} is used in place of the p_T of the neutrino, and $\Delta\phi(\ell, \nu)$ is the azimuthal angular difference between the directions of the lepton and neutrino.

For both top quark decays $t \rightarrow Hq \rightarrow b\bar{b}j$ and $t \rightarrow Wb \rightarrow b\ell\nu$, a full reconstruction of the top quark invariant mass m_{Hq} or m_{Wb} is possible. However, combinatorial background arises since there is no unambiguous way to match multiple light-quark and b quark jets with the final-state

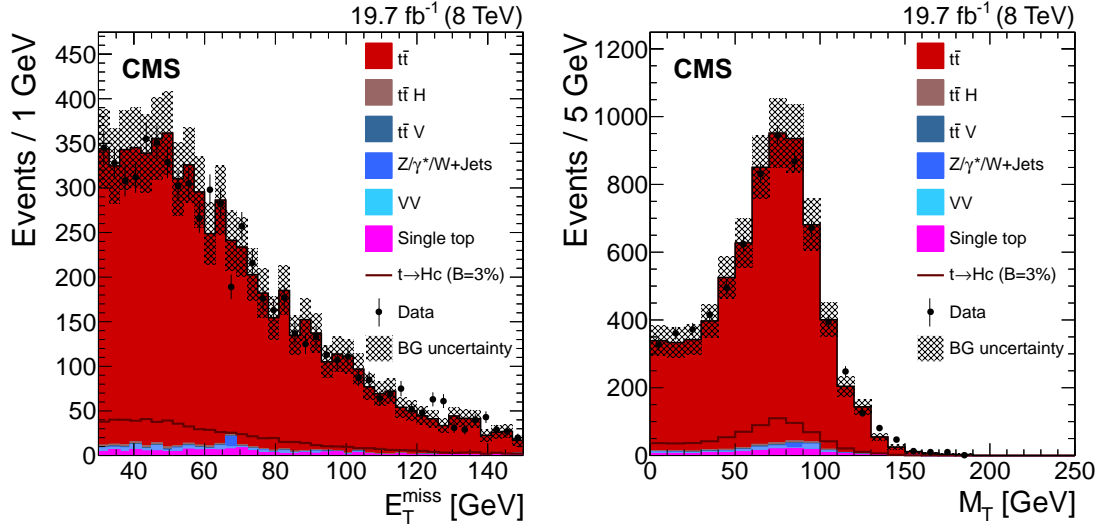


Figure 5: Comparison between data and simulated events after the basic selection for b jet + lepton events has been applied: the E_T^{miss} distribution (left) and the reconstructed transverse mass of the W boson candidate (right). A value of $\mathcal{B}(t \rightarrow Hc) = 3\%$ is used for the sake of improved visualization.

quarks. Therefore, all possible combinations are examined and a multivariate analysis (MVA) technique [51] is used to select the best candidate for each event. Several variables based on event kinematics and event topology are examined. Considering their signal-to-background separation power, the following variables are used to form a boosted decision tree (BDT) classifier [51]:

- the invariant masses m_{Hq} and m_{Hb} of the reconstructed top quarks,
- the energy of the u or c jet from the $t \rightarrow qH$ in the rest frame of its parent top quark,
- the azimuthal angle between the reconstructed top quarks directions,
- the azimuthal angle between the reconstructed W boson and the associated b jet directions,
- the azimuthal angle between the Higgs boson and the associated jet directions,
- the azimuthal angle between the directions of the b jets resulting from the Higgs boson decay.

The BDT classifier is trained with the correct and wrong combinations of simulated FCNC events determined from the generator-level parton matching. Because only event kinematics and topological variables are used, the Hu and Hc channels share the same BDT classifier. The jet-parton assignment in each event is determined by choosing the combination with the largest BDT classifier score, resulting in the correct assignment in 54% of events, as determined from simulation. The signal is determined using a template fit of the output of an artificial neural network (ANN) [51]. The ANN takes its inputs from the invariant mass of the reconstructed Higgs boson candidate and the CSV discriminator variables of the three b jets from the hadronic top quark and Higgs boson daughters. The training of the ANN is done separately for the $t \rightarrow Hu$ and $t \rightarrow Hc$ channels. A control sample dominated by $t\bar{t}$ is selected to validate the simulation used in the training. The sample is constructed by requiring one lepton and four

jets, of which exactly two are b jets.

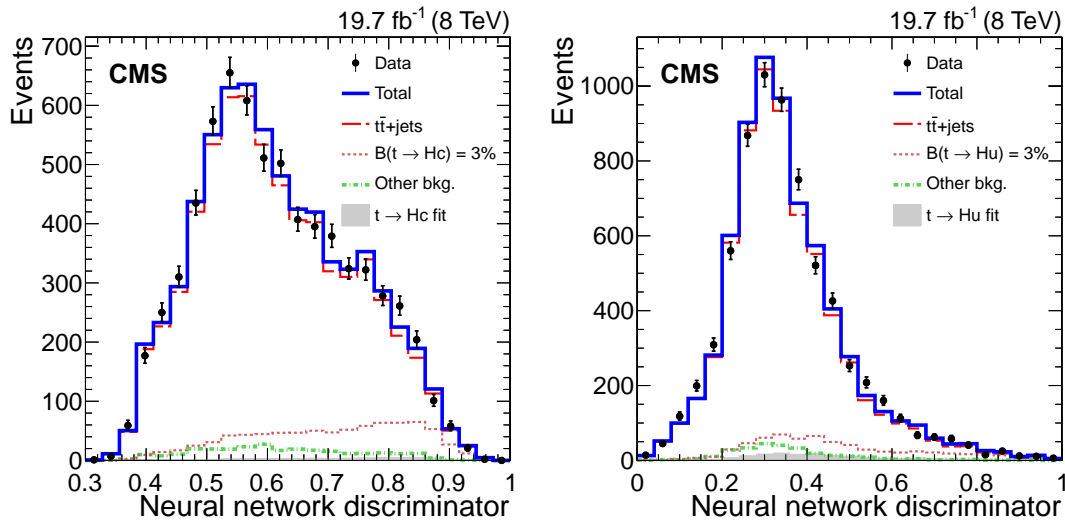


Figure 6: The output distributions from the ANN discriminator for data (points) and simulated background (lines) where the ANN was trained to discriminate the backgrounds from either $t \rightarrow Hc$ (left) or $t \rightarrow Hu$ (right) decays. The solid line shows the result of the fit of the signal and background templates to data. The dotted line gives the predicted signal distribution from simulation for $\mathcal{B}(t \rightarrow Hc) = 3\%$ and the filled histogram shows the proportion of signal estimated from the fit.

Figure 6 show the results of the fit performed with the 6840 observed events. The observed number of events and the expected yields of the signal and the main backgrounds estimated from simulation are shown in Table 5. The estimated background and signal based on the fit of the ANN discriminator output is shown in Table 6. The number of signal and background events from the fit result for the Hc channel are 74 ± 109 (stat) ± 24 (syst) and 6770 ± 130 (stat) ± 950 (syst), respectively. The corresponding yields for the Hu channel are 197 ± 87 (stat) ± 59 (syst) and 6640 ± 120 (stat) ± 800 (syst), respectively.

Table 5: The expected number of background and signal events for the b jet + lepton selection from simulation. The signal yields from the simulation of the signal assume $\mathcal{B}(t \rightarrow Hq) = 1\%$. Uncertainties combine both statistical and systematic components in quadrature.

Process	Predicted number of events
$t\bar{t}$	7100 ± 1500
$t\bar{t} H$	55 ± 11
$Wb\bar{b}$	71 ± 14
Total background	7226 ± 1500
$t \rightarrow Hc$	272 ± 90
$t \rightarrow Hu$	215 ± 65
Observed	6840

6 Systematic uncertainties

In the fit to the data, systematic uncertainties are treated as nuisance parameters. Each of them is assigned a log-normal or Gaussian pdf, which is included into the likelihood in a frequentist manner by interpreting it as signal arising from pseudo-measurement distributions. Nuisance

Table 6: The measured number of background and signal events for the b jet + lepton selection from fitting the ANN output trained on $t \rightarrow Hc$ and $t \rightarrow Hu$ final states. Uncertainties are statistical and systematic values, respectively. The observed number of events is shown in the last row.

Process	$t \rightarrow Hc$	$t \rightarrow Hu$
Background	$6770 \pm 130 \pm 950$	$6440 \pm 120 \pm 800$
Signal	$74 \pm 109 \pm 24$	$197 \pm 87 \pm 59$
Observed	6840	

parameters can affect either the signal yield, the shape of kinematic variable distributions, or both. If a specific source of uncertainty is not included for a given channel, it indicates that the uncertainty is either not applicable to that channel or is found to have negligible impact on the result.

The sources of uncertainties common to all analysis channels are: the uncertainty in the total integrated luminosity (2.6%) [52]; the effects of the event pileup modeling for the signal samples (0.2–3%), which is particularly important for the b jet + lepton channel; the uncertainty in the Higgs boson branching fractions (5%) [13]; the uncertainty in the $t\bar{t}$ cross section (7.5%) [53]; the uncertainty in the jet energy scale (1–15%) [29] and resolution (0.4–8%), where the larger uncertainty is for the b jet + lepton selection; the uncertainty in the PDF used in the event generators ($< 9\%$) [54]; the assumed top quark p_T distribution (1–4%) [43]; the E_T^{miss} resolution (0.2–4%) [29]; the uncertainty in the trigger efficiency ($< 2\%$); and the corrections applied to the simulation to account for the differences in lepton identification and isolation efficiencies in data and simulation (0.01–6%), where the larger uncertainty is for the selection of events with a three-electron final state.

The uncertainties specific to the signal description and background estimation for the multilepton analysis come from the 11–13% uncertainty in the $t\bar{t}W$ and $t\bar{t}Z$ theoretical cross sections [55]; the 15% uncertainty in the WZ normalization (determined from a control region); the uncertainty in the lepton misidentification rate (40% for electrons, 30% for muons); and the 20% uncertainty in the electron charge mismeasurement probability. The uncertainties specific to the signal description and background estimation for the diphoton channels are the corrections applied to the simulation to account for differences of the photon identification efficiency in data and simulation (0.1–5%); and the uncertainty in the jet and b jet identification efficiency (2–3.5%) [30]. The resonant background from the SM Higgs boson production has an uncertainty of 8.1% from the PDF uncertainty and 9.3% from the QCD scale [56].

The uncertainties specific to the signal description and background estimation for the b jet + lepton channel are dominated by the b jet identification. The uncertainty in the b tagging correction has two components: one is from the sample purity (4%) [30] and the other from the sample statistical uncertainty (24%). The uncertainty in the $t\bar{t}$ +jets cross section, determined using a leading-order event generator, is 1%. The uncertainty in the modeling of the heavy-flavor daughters of the W decay in the $t\bar{t}$ simulated sample is estimated to be 3%. Additional uncertainties arise from the event generator parameters such as the renormalization and factorization scales (5%) [41], the parton-jet matching threshold (1–9%), and the top quark mass (4%).

The uncertainties owing to the integrated luminosity, jet energy scale and resolution, pileup, reconstruction of physics objects, signal PDFs, and top quark related uncertainties are assumed to be fully correlated, while all others are treated as uncorrelated.

The systematic uncertainties are summarized in Table 7.

Table 7: Systematic uncertainties for the $t\bar{t} \rightarrow Hq + Wb$ ($q = u, c$) channels in percent. Ranges are quoted to indicate values that vary across the different analyses.

Channel	SS dilepton	Trilepton	$\gamma\gamma$ hadronic	$\gamma\gamma$ leptonic	b jet + lepton
Integrated luminosity	2.6	2.6	2.6	2.6	2.6
Pileup	1.0	1.0	0.3	0.8	0.2–3.0
Higgs boson branching fraction	5.0	5.0	5.0	5.0	5.0
$t\bar{t}$ cross section	7.5	7.5	7.5	7.5	7.5
Jet energy scale	0.5	0.6	1.2	1.0	5.2–15
Jet energy resolution	0.8	2.2	2.7	0.4	2.2–7.8
Signal PDF	6.0	6.0	5.9	5.2	<1–9.0
Top quark p_T correction	—	—	1.4	3.2	0.8–4.3
E_T^{miss}	4.0	4.0	—	—	0.2–2.5
Trigger efficiency	1.0–2.0	—	1.0	1.0	<0.1–0.4
Identification and isolation					
- muon	1.0–2.0	1.0–3.0	—	0.3	0.01–0.04
- electron	2.0–4.0	2.0–6.0	—	0.3	<0.1–0.2
$t\bar{t}W$ normalization	11.0	11.0	—	—	—
$t\bar{t}Z$ normalization	13.0	13.0	—	—	—
WZ normalization	15.0	15.0	—	—	—
Lepton misidentification					
- electron	40.0	40.0	—	—	—
- muon	30.0	30.0	—	—	—
Charge misidentification	20.0	—	—	—	—
Photon identification efficiency	—	—	5.2	5.2	—
Corrections per photon					
- energy scale	—	—	0.1	0.1	—
- energy resolution	—	—	0.1	0.1	—
- material mismodeling	—	—	0.3	0.3	—
- nonlinearity	—	—	0.1	0.1	—
Jet identification efficiency	—	—	2.0	2.0	—
b jet identification efficiency	—	—	2.9	3.5	—
Higgs boson background					
- cross section scale factors	—	—	9.3	9.3	—
- PDF	—	—	8.1	8.1	—
b jet CSV distribution					
- purity	—	—	—	—	1.0–3.4
- statistical precision	—	—	—	—	1.0–24
$t\bar{t}$ + heavy flavor jets	—	—	—	—	0.3–1.0
Modeling W decay daughters	—	—	—	—	1.6–2.7
Generator parameters					
- QCD scale	—	—	—	—	1.0–4.9
- matching parton-jet threshold	—	—	—	—	1.3–9.4
- top quark mass	—	—	—	—	0.8–4.1

7 Results

The expected number of events from the SM background processes and the expected number of signal events in data assuming a branching fraction $\mathcal{B}(t \rightarrow Hq) = 1\%$ are shown in Tables 3, 4,

and 6 for the multilepton, diphoton, and b jet + lepton selections, respectively. The final results are based on the combination of 12 channels: three SS dilepton, four trilepton, one diphoton + hadrons, two diphoton + lepton, and two b jet + lepton. The combination requires the simultaneous fit of the data selected by all the individual analyses, accounting for all statistical and systematic uncertainties, and their correlations. As $\mathcal{B}(t \rightarrow Hq)$ is expected to be small, the possibility of both top quarks decaying via FCNC is not considered.

No excess beyond the expected SM background is observed and upper limits at the 95% CL on the branching fractions of $t \rightarrow Hc$ and $t \rightarrow Hu$ are determined using the modified frequentist approach (asymptotic CLs method [57–59]). The observed 95% CL upper limits on the branching fractions $\mathcal{B}(t \rightarrow Hc)$ and $\mathcal{B}(t \rightarrow Hu)$ are 0.40% and 0.55%, respectively, obtained from the combined multilepton, diphoton, and b jet + lepton channels. A summary of the observed and expected limits is presented in Table 8. The diphoton channels are significantly more sensitive than the other channels, largely because of the lower uncertainty in the background model. The multilepton and b jet + lepton channels provide a 15% (37%) improvement on the observed (expected) upper limit when combined with the diphoton channel. A previous search for FCNC mediated by Higgs boson interactions via the $t \rightarrow Hc$ decay at the LHC made use of trilepton and diphoton final states [11]. The inclusion of new channels (SS dilepton, diphoton, and b jet + lepton final states) in addition to refinements in the trilepton and diphoton channels results in an improvement of 30% (34%) in the observed (expected) upper limit on $\mathcal{B}(t \rightarrow Hc)$.

The partial width of the $t \rightarrow Hq$ process is related to the square of the Yukawa coupling λ_{tq} by the formula [60, 61]:

$$\Gamma_{t \rightarrow Hq} = \frac{m_t}{16\pi} \left| \lambda_{tq}^H \right|^2 [(y_q + 1)^2 - y^2] \sqrt{1 - (y - y_q)^2} \sqrt{1 - (y + y_q)^2},$$

where $y = m_H/m_t$ and $y_q = m_q/m_t$. (Note that a convention where the parity of the coupling is ignored is adopted here: this introduces a factor of two when comparing to the ATLAS result.) Assuming the $t \rightarrow Wb$ partial width to be dominant, the upper limit on the $t \rightarrow Hq$ branching fractions can be translated into an upper limit on the square of the couplings using the relations:

$$\mathcal{B}(t \rightarrow Hc) = \Gamma_{t \rightarrow Hc} / \Gamma_{\text{Total}} = (0.58 \pm 0.01) \left| \lambda_{tc}^H \right|^2,$$

$$\mathcal{B}(t \rightarrow Hu) = \Gamma_{t \rightarrow Hu} / \Gamma_{\text{Total}} = (0.56 \pm 0.01) \left| \lambda_{tu}^H \right|^2,$$

where the CKM matrix element $|V_{tb}|$ is assumed to be equal to unity in the NLO order calculation [62] of $\Gamma_{\text{Total}} \approx \Gamma_{t \rightarrow Wb} = 1.372 \text{ GeV}$, and uncertainties arise from uncertainties on the mass values. The Particle Data Group [4] values of $m_H = 125 \text{ GeV}$, $m_t = 173.5 \text{ GeV}$, $m_c = 1.29 \text{ GeV}$, and $m_u = 2.3 \text{ MeV}$ are used.

Based on the analysis results, the observed (expected) 95% CL upper limits on the squares of the top-Higgs Yukawa couplings are:

$$\left| \lambda_{tc}^H \right|^2 < 6.9 (7.4_{-2.2}^{+3.6}) \times 10^{-3},$$

$$\left| \lambda_{tu}^H \right|^2 < 9.8 (7.1_{-2.3}^{+3.2}) \times 10^{-3}.$$

Table 8: The observed and expected upper limits at the 95% CL on the branching fraction (in %) of $t \rightarrow Hq$ ($q = u, c$) for: trilepton, SS dilepton, and combined multilepton channels; diphoton; b jet + lepton; and the combination of all channels. For the expected upper limit, the limit plus and minus a standard deviation are also shown.

	$\mathcal{B}_{\text{obs}}(t \rightarrow Hc)$	$\mathcal{B}_{\text{exp}}(t \rightarrow Hc)$	$\mathcal{B}_{\text{exp}+\sigma}$	$\mathcal{B}_{\text{exp}-\sigma}$
Trilepton	1.26	1.33	1.87	0.95
Same-sign dilepton	0.99	0.93	1.26	0.68
Multilepton combined	0.93	0.89	1.22	0.65
Diphoton hadronic	1.26	1.33	1.87	0.95
Diphoton leptonic	0.99	0.93	1.26	0.68
Diphoton combined	0.47	0.67	1.06	0.44
b jet + lepton	1.16	0.89	1.37	0.60
Full combination	0.40	0.43	0.64	0.30
	$\mathcal{B}_{\text{obs}}(t \rightarrow Hu)$	$\mathcal{B}_{\text{exp}}(t \rightarrow Hu)$	$\mathcal{B}_{\text{exp}+\sigma}$	$\mathcal{B}_{\text{exp}-\sigma}$
Trilepton	1.34	1.47	2.09	1.05
Same-sign dilepton	0.93	0.85	1.16	0.62
Multilepton combined	0.86	0.82	1.14	0.60
Diphoton hadronic	1.26	1.33	1.87	0.95
Diphoton leptonic	0.99	0.93	1.26	0.68
Diphoton combined	0.42	0.60	0.96	0.39
b jet + lepton	1.92	0.84	1.31	0.57
Full combination	0.55	0.40	0.58	0.27

8 Summary

A search for flavor-changing neutral currents in the decay of a top quark to a charm or up quark and a Higgs boson based on $\sqrt{s} = 8$ TeV proton-proton collisions has been presented. Samples of multilepton, diphoton, and b jet + lepton events were selected from data recorded with the CMS detector, corresponding to an integrated luminosity of 19.7 fb^{-1} . The topologies $pp \rightarrow t\bar{t} \rightarrow Hq + Wb$ events, where $q = u, c$ and H is allowed to decay into $WW, ZZ, \tau\tau, \gamma\gamma$, and $b\bar{b}$. No excess of events above the SM background is observed, and branching fractions of $\mathcal{B}(t \rightarrow Hc)$ larger than 0.40% and $\mathcal{B}(t \rightarrow Hu)$ larger than 0.55% are excluded at the 95% confidence level. These observed upper limits on $\mathcal{B}(t \rightarrow Hq)$ and the corresponding constraints on the top quark flavor-changing Higgs boson Yukawa couplings are amongst the most stringent measured to date.

Acknowledgments

We congratulate our colleagues in the CERN accelerator departments for the excellent performance of the LHC and thank the technical and administrative staffs at CERN and at other CMS institutes for their contributions to the success of the CMS effort. In addition, we gratefully acknowledge the computing centers and personnel of the Worldwide LHC Computing Grid for delivering so effectively the computing infrastructure essential to our analyses. Finally, we acknowledge the enduring support for the construction and operation of the LHC and the CMS detector provided by the following funding agencies: the Austrian Federal Ministry of Science, Research and Economy and the Austrian Science Fund; the Belgian Fonds de la Recherche Scientifique, and Fonds voor Wetenschappelijk Onderzoek; the Brazilian Funding Agencies (CNPq, CAPES, FAPERJ, and FAPESP); the Bulgarian Ministry of Education and

Science; CERN; the Chinese Academy of Sciences, Ministry of Science and Technology, and National Natural Science Foundation of China; the Colombian Funding Agency (COLCIENCIAS); the Croatian Ministry of Science, Education and Sport, and the Croatian Science Foundation; the Research Promotion Foundation, Cyprus; the Secretariat for Higher Education, Science, Technology and Innovation, Ecuador; the Ministry of Education and Research, Estonian Research Council via IUT23-4 and IUT23-6 and European Regional Development Fund, Estonia; the Academy of Finland, Finnish Ministry of Education and Culture, and Helsinki Institute of Physics; the Institut National de Physique Nucléaire et de Physique des Particules / CNRS, and Commissariat à l'Énergie Atomique et aux Énergies Alternatives / CEA, France; the Bundesministerium für Bildung und Forschung, Deutsche Forschungsgemeinschaft, and Helmholtz-Gemeinschaft Deutscher Forschungszentren, Germany; the General Secretariat for Research and Technology, Greece; the National Scientific Research Foundation, and National Innovation Office, Hungary; the Department of Atomic Energy and the Department of Science and Technology, India; the Institute for Studies in Theoretical Physics and Mathematics, Iran; the Science Foundation, Ireland; the Istituto Nazionale di Fisica Nucleare, Italy; the Ministry of Science, ICT and Future Planning, and National Research Foundation (NRF), Republic of Korea; the Lithuanian Academy of Sciences; the Ministry of Education, and University of Malaya (Malaysia); the Mexican Funding Agencies (BUAP, CINVESTAV, CONACYT, LNS, SEP, and UASLP-FAI); the Ministry of Business, Innovation and Employment, New Zealand; the Pakistan Atomic Energy Commission; the Ministry of Science and Higher Education and the National Science Centre, Poland; the Fundação para a Ciência e a Tecnologia, Portugal; JINR, Dubna; the Ministry of Education and Science of the Russian Federation, the Federal Agency of Atomic Energy of the Russian Federation, Russian Academy of Sciences, and the Russian Foundation for Basic Research; the Ministry of Education, Science and Technological Development of Serbia; the Secretaría de Estado de Investigación, Desarrollo e Innovación and Programa Consolider-Ingenio 2010, Spain; the Swiss Funding Agencies (ETH Board, ETH Zurich, PSI, SNF, UniZH, Canton Zurich, and SER); the Ministry of Science and Technology, Taipei; the Thailand Center of Excellence in Physics, the Institute for the Promotion of Teaching Science and Technology of Thailand, Special Task Force for Activating Research and the National Science and Technology Development Agency of Thailand; the Scientific and Technical Research Council of Turkey, and Turkish Atomic Energy Authority; the National Academy of Sciences of Ukraine, and State Fund for Fundamental Researches, Ukraine; the Science and Technology Facilities Council, UK; the US Department of Energy, and the US National Science Foundation.

Individuals have received support from the Marie-Curie program and the European Research Council and EPLANET (European Union); the Leventis Foundation; the A. P. Sloan Foundation; the Alexander von Humboldt Foundation; the Belgian Federal Science Policy Office; the Fonds pour la Formation à la Recherche dans l'Industrie et dans l'Agriculture (FRIA-Belgium); the Agentschap voor Innovatie door Wetenschap en Technologie (IWT-Belgium); the Ministry of Education, Youth and Sports (MEYS) of the Czech Republic; the Council of Science and Industrial Research, India; the HOMING PLUS program of the Foundation for Polish Science, cofinanced from European Union, Regional Development Fund, the Mobility Plus program of the Ministry of Science and Higher Education, the National Science Center (Poland), contracts Harmonia 2014/14/M/ST2/00428, Opus 2013/11/B/ST2/04202, 2014/13/B/ST2/02543 and 2014/15/B/ST2/03998, Sonata-bis 2012/07/E/ST2/01406; the Thalys and Aristeia programs cofinanced by EU-ESF and the Greek NSRF; the National Priorities Research Program by Qatar National Research Fund; the Programa Clarín-COFUND del Principado de Asturias; the Rachadapisek Sompot Fund for Postdoctoral Fellowship, Chulalongkorn University and the Chulalongkorn Academic into Its 2nd Century Project Advancement Project (Thailand); and the Welch Foundation, contract C-1845.

References

- [1] ATLAS Collaboration, "Observation of a new particle in the search for the Standard Model Higgs boson with the ATLAS detector at the LHC", *Phys. Lett. B* **716** (2012) 1, doi:10.1016/j.physletb.2012.08.020, arXiv:1207.7214.
- [2] CMS Collaboration, "Observation of a new boson at a mass of 125 GeV with the CMS experiment at the LHC", *Phys. Lett. B* **716** (2012) 30, doi:10.1016/j.physletb.2012.08.021, arXiv:1207.7235.
- [3] CMS Collaboration, "Observation of a new boson with mass near 125 GeV in pp collisions at $\sqrt{s} = 7$ and 8 TeV", *JHEP* **06** (2013) 081, doi:10.1007/JHEP06(2013)081, arXiv:1303.4571.
- [4] Particle Data Group, K. A. Olive et al., "Review of Particle Physics", *Chin. Phys. C* **38** (2014) 090001, doi:10.1088/1674-1137/38/9/090001.
- [5] M. Czakon, P. Fiedler, and A. Mitov, "Total Top-Quark Pair-Production Cross Section at Hadron Colliders Through $O(\alpha_s^4)$ ", *Phys. Rev. Lett.* **110** (2013) 252004, doi:10.1103/PhysRevLett.110.252004, arXiv:1303.6254.
- [6] G. Eilam, J. L. Hewett, and A. Soni, "Rare decays of the top quark in the standard and two Higgs doublet models", *Phys. Rev. D* **44** (1991) 1473, doi:10.1103/PhysRevD.44.1473. [Erratum: doi:10.1103/PhysRevD.59.039901].
- [7] B. Mele, S. Petrarca, and A. Soddu, "A new evaluation of the $t \rightarrow cH$ decay width in the standard model", *Phys. Lett. B* **435** (1998) 401, doi:10.1016/S0370-2693(98)00822-3, arXiv:hep-ph/9805498.
- [8] J. A. Aguilar-Saavedra, "Top flavor-changing neutral interactions: Theoretical expectations and experimental detection", *Acta Phys. Polon. B* **35** (2004) 2695, arXiv:hep-ph/0409342.
- [9] ATLAS Collaboration, "Search for top quark decays $t \rightarrow qH$ with $H \rightarrow \gamma\gamma$ using the ATLAS detector", *JHEP* **06** (2014) 008, doi:10.1007/JHEP06(2014)008, arXiv:1403.6293.
- [10] ATLAS Collaboration, "Search for flavour-changing neutral current top quark decays $t \rightarrow Hq$ in pp collisions at $\sqrt{s} = 8$ TeV with the ATLAS detector", *JHEP* **12** (2015) 061, doi:10.1007/JHEP12(2015)061, arXiv:1509.06047.
- [11] CMS Collaboration, "Searches for heavy Higgs bosons in two-Higgs-doublet models and for t to ch decay using multilepton and diphoton final states in pp collisions at 8 TeV", *Phys. Rev. D* **90** (2014) 112013, doi:10.1103/PhysRevD.90.112013, arXiv:1410.2751.
- [12] LHC Higgs Cross Section Working Group, "Handbook of LHC Higgs Cross Sections: 3. Higgs Properties", (2013). arXiv:1307.1347.
- [13] A. Denner et al., "Standard model Higgs-boson branching ratios with uncertainties", *Eur. Phys. J. C* **71** (2011) 1753, doi:10.1140/epjc/s10052-011-1753-8, arXiv:1107.5909.

- [14] CMS Collaboration, “The CMS experiment at the CERN LHC”, *JINST* **3** (2008) S08004, doi:10.1088/1748-0221/3/08/S08004.
- [15] CMS Collaboration, “Performance of Photon Reconstruction and Identification with the CMS Detector in Proton-Proton Collisions at $\sqrt{s} = 8$ TeV”, *JINST* **10** (2015) P08010, doi:10.1088/1748-0221/10/08/P08010, arXiv:1502.02702.
- [16] CMS Collaboration, “Particle-Flow Event Reconstruction in CMS and Performance for Jets, Taus, and E_T^{miss} ”, CMS Physics Analysis Summary CMS-PAS-PFT-09-001, 2009.
- [17] CMS Collaboration, “Commissioning of the Particle-Flow Event Reconstruction with the first LHC collisions recorded in the CMS detector”, CMS Physics Analysis Summary CMS-PAS-PFT-10-001, 2010.
- [18] S. Baffioni et al., “Electron reconstruction in CMS”, *Eur. Phys. J. C* **49** (2007) 1099, doi:10.1140/epjc/s10052-006-0175-5.
- [19] CMS Collaboration, “Performance of CMS muon reconstruction in pp collision events at $\sqrt{s} = 7$ TeV”, *JINST* **7** (2012) P10002, doi:10.1088/1748-0221/7/10/P10002, arXiv:1206.4071.
- [20] CMS Collaboration, “Performance of electron reconstruction and selection with the CMS detector in proton-proton collisions at $\sqrt{s} = 8$ TeV”, *JINST* **10** (2015) P06005, doi:10.1088/1748-0221/10/06/P06005, arXiv:1502.02701.
- [21] CMS Collaboration, “Study of the mass and spin-parity of the Higgs boson candidate via its decays to Z boson pairs”, *Phys. Rev. Lett.* **110** (2013) 81803, doi:10.1103/PhysRevLett.110.081803, arXiv:1212.6639.
- [22] CMS Collaboration, “Energy calibration and resolution of the CMS electromagnetic calorimeter in pp collisions at $\sqrt{s} = 7$ TeV”, *JINST* **8** (2013) P09009, doi:10.1088/1748-0221/8/09/P09009, arXiv:1306.2016.
- [23] CMS Collaboration, “Observation of the diphoton decay of the Higgs boson and measurement of its properties”, *Eur. Phys. J. C* **74** (2014) 3076, doi:10.1140/epjc/s10052-014-3076-z, arXiv:1407.0558.
- [24] CMS Collaboration, “Measurement of the inclusive W and Z production cross sections in pp collisions at $\sqrt{s} = 7$ TeV”, *JHEP* **10** (2011) 132, doi:10.1007/JHEP10(2011)132, arXiv:1107.4789.
- [25] M. Cacciari and G. P. Salam, “Dispelling the N^3 myth for the k_t jet-finder”, *Phys. Lett. B* **641** (2006) 57, doi:10.1016/j.physletb.2006.08.037, arXiv:hep-ph/0512210.
- [26] M. Cacciari and G. P. Salam, “Pileup subtraction using jet areas”, *Phys. Lett. B* **659** (2008) 119, doi:10.1016/j.physletb.2007.09.077, arXiv:0707.1378.
- [27] M. Cacciari, G. P. Salam, and G. Soyez, “The Catchment Area of Jets”, *JHEP* **04** (2008) 005, doi:10.1088/1126-6708/2008/04/005, arXiv:0802.1188.
- [28] M. Cacciari, G. P. Salam, and G. Soyez, “FastJet User Manual”, *Eur. Phys. J. C* **72** (2012) 1896, doi:10.1140/epjc/s10052-012-1896-2, arXiv:1111.6097.
- [29] CMS Collaboration, “Determination of jet energy calibration and transverse momentum resolution in CMS”, *JINST* **6** (2011) 11002, doi:10.1088/1748-0221/6/11/P11002, arXiv:1107.4277.

- [30] CMS Collaboration, “Identification of b-quark jets with the CMS experiment”, *JINST* **8** (2013) P04013, doi:10.1088/1748-0221/8/04/P04013, arXiv:1211.4462.
- [31] J. Alwall et al., “MadGraph 5: Going Beyond”, *JHEP* **06** (2011) 128, doi:10.1007/JHEP06(2011)128, arXiv:1106.0522.
- [32] P. Nason, “A new method for combining NLO QCD with shower Monte Carlo algorithms”, *JHEP* **11** (2004) 040, doi:10.1088/1126-6708/2004/11/040, arXiv:hep-ph/0409146.
- [33] S. Frixione et al., “Matching NLO QCD computations with parton shower simulations: the POWHEG method”, *JHEP* **11** (2007) 070, doi:10.1088/1126-6708/2007/11/070, arXiv:0709.2092.
- [34] S. Alioli et al., “A general framework for implementing NLO calculations in shower Monte Carlo programs: the POWHEG BOX”, *JHEP* **06** (2010) 043, doi:10.1007/JHEP06(2010)043, arXiv:1002.2581.
- [35] T. Sjöstrand, S. Mrenna, and P. Skands, “PYTHIA 6.4 physics and manual”, *JHEP* **05** (2006) 026, doi:10.1088/1126-6708/2006/05/026, arXiv:hep-ph/0603175.
- [36] Z. Was, “TAUOLA the library for tau lepton decay, and KKMC / KORALB / KORALZ /... status report”, *Nucl. Phys. Proc. Suppl.* **98** (2001) 96, doi:10.1016/S0920-5632(01)01200-2, arXiv:hep-ph/0011305.
- [37] T. Gleisberg et al., “Event generation with SHERPA 1.1”, *JHEP* **02** (2009) 007, doi:10.1088/1126-6708/2009/02/007, arXiv:0811.4622.
- [38] J. Reuter et al., “Modern Particle Physics Event Generation with WHIZARD”, *J. Phys. Conf. Ser.* **608** (2015) 012063, doi:10.1088/1742-6596/608/1/012063, arXiv:1410.4505.
- [39] R. Field, “Min-Bias and the Underlying Event at the LHC”, *Acta Phys. Polon. B* **42** (2011) 2631, doi:10.5506/APhysPolB.42.2631, arXiv:1110.5530.
- [40] H.-L. Lai et al., “Uncertainty induced by QCD coupling in the CTEQ global analysis of parton distributions”, *Phys. Rev. D* **82** (2010) 054021, doi:10.1103/PhysRevD.82.054021, arXiv:1004.4624.
- [41] P. M. Nadolsky et al., “Implications of CTEQ global analysis for collider observables”, *Phys. Rev. D* **78** (2008) 013004, doi:10.1103/PhysRevD.78.013004, arXiv:0802.0007.
- [42] GEANT4 Collaboration, “GEANT4 – a simulation toolkit”, *Nucl. Instrum. Meth. A* **506** (2003) 250, doi:10.1016/S0168-9002(03)01368-8.
- [43] CMS Collaboration, “Measurement of the differential cross section for top quark pair production in pp collisions at $\sqrt{s} = 8$ TeV”, *Eur. Phys. J. C* **75** (2015) 542, doi:10.1140/epjc/s10052-015-3709-x, arXiv:1505.04480.
- [44] CMS Collaboration, “Search for the associated production of the Higgs boson with a top-quark pair”, *JHEP* **09** (2014) 087, doi:10.1007/JHEP09(2014)087, arXiv:1408.1682. [Erratum: doi:10.1007/JHEP10(2014)106.]

- [45] CMS Collaboration, “Measurement of the Drell-Yan cross section in pp collisions at $\sqrt{s} = 7$ TeV”, *JHEP* **10** (2011) 007, doi:10.1007/JHEP10(2011)007, arXiv:1108.0566.
- [46] R. C. Gray et al., “Backgrounds To Higgs Boson Searches from $W\gamma^* \rightarrow l\nu(l)$ Asymmetric Internal Conversion”, (2011). arXiv:1110.1368.
- [47] CMS Collaboration, “Search for new physics with same-sign isolated dilepton events with jets and missing transverse energy at the LHC”, *JHEP* **06** (2011) 077, doi:10.1007/JHEP06(2011)077, arXiv:1104.3168.
- [48] CMS Collaboration, “Search for new physics with same-sign isolated dilepton events with jets and missing transverse energy”, *Phys. Rev. Lett.* **109** (2012) 071803, doi:10.1103/PhysRevLett.109.071803, arXiv:1205.6615.
- [49] CMS Collaboration, “Search for the standard model Higgs boson decaying to W^+W^- in the fully leptonic final state in pp collisions at $\sqrt{s} = 7$ TeV”, *Phys. Lett. B* **710** (2012) 91, doi:10.1016/j.physletb.2012.02.076, arXiv:1202.1489.
- [50] CMS Collaboration, “Search for the standard model Higgs boson decaying into two photons in pp collisions at $\sqrt{s} = 7$ TeV”, *Phys. Lett. B* **710** (2012) 403, doi:10.1016/j.physletb.2012.03.003, arXiv:1202.1487.
- [51] H. Voss, A. Höcker, J. Stelzer, and F. Tegenfeldt, “TMVA, the Toolkit for Multivariate Data Analysis with ROOT”, in *XIth International Workshop on Advanced Computing and Analysis Techniques in Physics Research (ACAT)*, p. 40. 2007. arXiv:physics/0703039.
- [52] CMS Collaboration, “CMS Luminosity Based on Pixel Cluster Counting - Summer 2013 Update”, CMS Physics Analysis Summary CMS-PAS-LUM-13-001, 2013.
- [53] CMS Collaboration, “Measurement of the $t\bar{t}$ production cross section in pp collisions at $\sqrt{s} = 8$ TeV in dilepton final states containing one τ lepton”, *Phys. Lett. B* **739** (2014) 23, doi:10.1016/j.physletb.2014.10.032, arXiv:1407.6643.
- [54] D. Bourilkov, R. C. Group, and M. R. Whalley, “LHAPDF: PDF use from the Tevatron to the LHC”, in *TeV4LHC Workshop - 4th meeting Batavia, Illinois, October 20-22, 2005*. 2006. arXiv:hep-ph/0605240.
- [55] M. V. Garzelli, A. Kardos, C. G. Papadopoulos, and Z. Trocsanyi, “ $t\bar{t} W^\pm$ and $t\bar{t} Z$ hadroproduction at NLO accuracy in QCD with parton shower and hadronization effects”, *JHEP* **11** (2012) 056, doi:10.1007/JHEP11(2012)056, arXiv:1208.2665.
- [56] LHC Higgs Cross Section Working Group Collaboration, “Handbook of LHC Higgs Cross Sections: 1. Inclusive Observables”, (2011). arXiv:1101.0593.
- [57] T. Junk, “Confidence level computation for combining searches with small statistics”, *Nucl. Instrum. Meth. A* **434** (1999) 435, doi:10.1016/S0168-9002(99)00498-2, arXiv:hep-ex/9902006.
- [58] A. L. Read, “Presentation of search results: the CL_s technique”, *J. Phys. G* **28** (2002) 2693, doi:10.1088/0954-3899/28/10/313.
- [59] G. Cowan, K. Cranmer, E. Gross, and O. Vitells, “Asymptotic formulae for likelihood-based tests of new physics”, *Eur. Phys. J. C* **71** (2011) 1554, doi:10.1140/epjc/s10052-011-1554-0, arXiv:1007.1727. [Erratum: doi:10.1140/epjc/s10052-013-2501-z].

-
- [60] N. Craig et al., “Searching for $t \rightarrow ch$ with Multi-Leptons”, *Phys. Rev. D* **86** (2012) 075002, doi:10.1103/PhysRevD.86.075002, arXiv:1207.6794.
- [61] D. Atwood, S. K. Gupta, and A. Soni, “Constraining the flavor changing Higgs couplings to the top-quark at the LHC”, *JHEP* **10** (2014) 057, doi:10.1007/JHEP10(2014)057, arXiv:1305.2427.
- [62] A. Denner and T. Sack, “The top width”, *Nucl. Phys. B* **358** (1991) 46, doi:10.1016/0550-3213(91)90530-B.

A The CMS Collaboration

Yerevan Physics Institute, Yerevan, Armenia

V. Khachatryan, A.M. Sirunyan, A. Tumasyan

Institut für Hochenergiephysik, Wien, Austria

W. Adam, E. Asilar, T. Bergauer, J. Brandstetter, E. Brondolin, M. Dragicevic, J. Erö, M. Flechl, M. Friedl, R. Frühwirth¹, V.M. Ghete, C. Hartl, N. Hörmann, J. Hrubec, M. Jeitler¹, A. König, I. Krätschmer, D. Liko, T. Matsushita, I. Mikulec, D. Rabadý, N. Rad, B. Rahbaran, H. Rohringer, J. Schieck¹, J. Strauss, W. Treberer-Treberspurg, W. Waltenberger, C.-E. Wulz¹

National Centre for Particle and High Energy Physics, Minsk, Belarus

V. Mossolov, N. Shumeiko, J. Suarez Gonzalez

Universiteit Antwerpen, Antwerpen, Belgium

S. Alderweireldt, E.A. De Wolf, X. Janssen, A. Knutsson, J. Lauwers, M. Van De Klundert, H. Van Haevermaet, P. Van Mechelen, N. Van Remortel, A. Van Spilbeeck

Vrije Universiteit Brussel, Brussel, Belgium

S. Abu Zeid, F. Blekman, J. D'Hondt, N. Daci, I. De Bruyn, K. Deroover, N. Heracleous, S. Lowette, S. Moortgat, L. Moreels, A. Olbrechts, Q. Python, S. Tavernier, W. Van Doninck, P. Van Mulders, I. Van Parijs

Université Libre de Bruxelles, Bruxelles, Belgium

H. Brun, C. Caillol, B. Clerbaux, G. De Lentdecker, H. Delannoy, G. Fasanella, L. Favart, R. Goldouzian, A. Grebenyuk, G. Karapostoli, T. Lenzi, A. Léonard, J. Luetic, T. Maerschalk, A. Marinov, A. Randle-conde, T. Seva, C. Vander Velde, P. Vanlaer, R. Yonamine, F. Zenoni, F. Zhang²

Ghent University, Ghent, Belgium

A. Cimmino, T. Cornelis, D. Dobur, A. Fagot, G. Garcia, M. Gul, J. Mccartin, D. Poyraz, S. Salva, R. Schöfbeck, M. Tytgat, W. Van Driessche, E. Yazgan, N. Zaganidis

Université Catholique de Louvain, Louvain-la-Neuve, Belgium

C. Beluffi³, O. Bondu, S. Brochet, G. Bruno, A. Caudron, L. Ceard, S. De Visscher, C. Delaere, M. Delcourt, L. Forthomme, B. Francois, A. Giammanco, A. Jafari, P. Jez, M. Komm, V. Lemaitre, A. Magitteri, A. Mertens, M. Musich, C. Nuttens, K. Piotrkowski, L. Quertenmont, M. Selvaggi, M. Vidal Marono, S. Wertz

Université de Mons, Mons, Belgium

N. Bely

Centro Brasileiro de Pesquisas Fisicas, Rio de Janeiro, Brazil

W.L. Aldá Júnior, F.L. Alves, G.A. Alves, L. Brito, M. Correa Martins Junior, C. Hensel, A. Moraes, M.E. Pol, P. Rebello Teles

Universidade do Estado do Rio de Janeiro, Rio de Janeiro, Brazil

E. Belchior Batista Das Chagas, W. Carvalho, J. Chinellato⁴, A. Custódio, E.M. Da Costa, G.G. Da Silveira, D. De Jesus Damiao, C. De Oliveira Martins, S. Fonseca De Souza, L.M. Huertas Guativa, H. Malbouisson, D. Matos Figueiredo, C. Mora Herrera, L. Mundim, H. Nogima, W.L. Prado Da Silva, A. Santoro, A. Sznajder, E.J. Tonelli Manganote⁴, A. Vilela Pereira

Universidade Estadual Paulista ^a, Universidade Federal do ABC ^b, São Paulo, Brazil

S. Ahuja^a, C.A. Bernardes^b, S. Dogra^a, T.R. Fernandez Perez Tomei^a, E.M. Gregores^b,

P.G. Mercadante^b, C.S. Moon^{a,5}, S.F. Novaes^a, Sandra S. Padula^a, D. Romero Abad^b, J.C. Ruiz Vargas

Institute for Nuclear Research and Nuclear Energy, Sofia, Bulgaria

A. Aleksandrov, R. Hadjiiska, P. Iaydjiev, M. Rodozov, S. Stoykova, G. Sultanov, M. Vutova

University of Sofia, Sofia, Bulgaria

A. Dimitrov, I. Glushkov, L. Litov, B. Pavlov, P. Petkov

Beihang University, Beijing, China

W. Fang⁶

Institute of High Energy Physics, Beijing, China

M. Ahmad, J.G. Bian, G.M. Chen, H.S. Chen, M. Chen, Y. Chen⁷, T. Cheng, R. Du, C.H. Jiang, D. Leggat, Z. Liu, F. Romeo, S.M. Shaheen, A. Spiezia, J. Tao, C. Wang, Z. Wang, H. Zhang, J. Zhao

State Key Laboratory of Nuclear Physics and Technology, Peking University, Beijing, China

C. Asawatangtrakuldee, Y. Ban, Q. Li, S. Liu, Y. Mao, S.J. Qian, D. Wang, Z. Xu

Universidad de Los Andes, Bogota, Colombia

C. Avila, A. Cabrera, L.F. Chaparro Sierra, C. Florez, J.P. Gomez, C.F. González Hernández, J.D. Ruiz Alvarez, J.C. Sanabria

University of Split, Faculty of Electrical Engineering, Mechanical Engineering and Naval Architecture, Split, Croatia

N. Godinovic, D. Lelas, I. Puljak, P.M. Ribeiro Cipriano

University of Split, Faculty of Science, Split, Croatia

Z. Antunovic, M. Kovac

Institute Rudjer Boskovic, Zagreb, Croatia

V. Brigljevic, D. Ferencek, K. Kadija, S. Micanovic, L. Sudic

University of Cyprus, Nicosia, Cyprus

A. Attikis, G. Mavromanolakis, J. Mousa, C. Nicolaou, F. Ptochos, P.A. Razis, H. Rykaczewski

Charles University, Prague, Czech Republic

M. Finger⁸, M. Finger Jr.⁸

Universidad San Francisco de Quito, Quito, Ecuador

E. Carrera Jarrin

Academy of Scientific Research and Technology of the Arab Republic of Egypt, Egyptian Network of High Energy Physics, Cairo, Egypt

A.A. Abdelalim^{9,10}, E. El-khateeb¹¹, M.A. Mahmoud^{12,13}, A. Radi^{13,11}

National Institute of Chemical Physics and Biophysics, Tallinn, Estonia

B. Calpas, M. Kadastik, M. Murumaa, L. Perrini, M. Raidal, A. Tiko, C. Veelken

Department of Physics, University of Helsinki, Helsinki, Finland

P. Eerola, J. Pekkanen, M. Voutilainen

Helsinki Institute of Physics, Helsinki, Finland

J. Härkönen, V. Karimäki, R. Kinnunen, T. Lampén, K. Lassila-Perini, S. Lehti, T. Lindén, P. Luukka, T. Peltola, J. Tuominiemi, E. Tuovinen, L. Wendland

Lappeenranta University of Technology, Lappeenranta, Finland

J. Talvitie, T. Tuuva

IRFU, CEA, Université Paris-Saclay, Gif-sur-Yvette, France

M. Besancon, F. Couderc, M. Dejardin, D. Denegri, B. Fabbro, J.L. Faure, C. Favaro, F. Ferri, S. Ganjour, S. Ghosh, A. Givernaud, P. Gras, G. Hamel de Monchenault, P. Jarry, I. Kucher, E. Locci, M. Machet, J. Malcles, J. Rander, A. Rosowsky, M. Titov, A. Zghiche

Laboratoire Leprince-Ringuet, Ecole Polytechnique, IN2P3-CNRS, Palaiseau, France

A. Abdulsalam, I. Antropov, S. Baffioni, F. Beaudette, P. Busson, L. Cadamuro, E. Chapon, C. Charlot, O. Davignon, R. Granier de Cassagnac, M. Jo, S. Lisniak, P. Miné, I.N. Naranjo, M. Nguyen, C. Ochando, G. Ortona, P. Paganini, P. Pigard, S. Regnard, R. Salerno, Y. Sirois, T. Strebler, Y. Yilmaz, A. Zabi

Institut Pluridisciplinaire Hubert Curien, Université de Strasbourg, Université de Haute Alsace Mulhouse, CNRS/IN2P3, Strasbourg, FranceJ.-L. Agram¹⁴, J. Andrea, A. Aubin, D. Bloch, J.-M. Brom, M. Buttignol, E.C. Chabert, N. Chanon, C. Collard, E. Conte¹⁴, X. Coubez, J.-C. Fontaine¹⁴, D. Gelé, U. Goerlach, A.-C. Le Bihan, J.A. Merlin¹⁵, K. Skovpen, P. Van Hove**Centre de Calcul de l'Institut National de Physique Nucleaire et de Physique des Particules, CNRS/IN2P3, Villeurbanne, France**

S. Gadrat

Université de Lyon, Université Claude Bernard Lyon 1, CNRS-IN2P3, Institut de Physique Nucléaire de Lyon, Villeurbanne, FranceS. Beauceron, C. Bernet, G. Boudoul, E. Bouvier, C.A. Carrillo Montoya, R. Chierici, D. Contardo, B. Courbon, P. Depasse, H. El Mamouni, J. Fan, J. Fay, S. Gascon, M. Gouzevitch, G. Grenier, B. Ille, F. Lagarde, I.B. Laktineh, M. Lethuillier, L. Mirabito, A.L. Pequegnot, S. Perries, A. Popov¹⁶, D. Sabes, V. Sordini, M. Vander Donckt, P. Verdier, S. Viret**Georgian Technical University, Tbilisi, Georgia**T. Toriashvili¹⁷**Tbilisi State University, Tbilisi, Georgia**Z. Tsamalaidze⁸**RWTH Aachen University, I. Physikalisches Institut, Aachen, Germany**C. Autermann, S. Beranek, L. Feld, A. Heister, M.K. Kiesel, K. Klein, M. Lipinski, A. Ostapchuk, M. Preuten, F. Raupach, S. Schael, C. Schomakers, J.F. Schulte, J. Schulz, T. Verlage, H. Weber, V. Zhukov¹⁶**RWTH Aachen University, III. Physikalisches Institut A, Aachen, Germany**

M. Brodski, E. Dietz-Laursonn, D. Duchardt, M. Endres, M. Erdmann, S. Erdweg, T. Esch, R. Fischer, A. Güth, T. Hebbeker, C. Heidemann, K. Hoepfner, S. Knutzen, M. Merschmeyer, A. Meyer, P. Millet, S. Mukherjee, M. Olschewski, K. Padeken, P. Papacz, T. Pook, M. Radziej, H. Reithler, M. Rieger, F. Scheuch, L. Sonnenschein, D. Teyssier, S. Thüer

RWTH Aachen University, III. Physikalisches Institut B, Aachen, GermanyV. Cherepanov, Y. Erdogan, G. Flügge, F. Hoehle, B. Kargoll, T. Kress, A. Künsken, J. Lingemann, A. Nehr Korn, A. Nowack, I.M. Nugent, C. Pistone, O. Pooth, A. Stahl¹⁵**Deutsches Elektronen-Synchrotron, Hamburg, Germany**M. Aldaya Martin, I. Asin, K. Beernaert, O. Behnke, U. Behrens, A.A. Bin Anuar, K. Borras¹⁸, A. Campbell, P. Connor, C. Contreras-Campana, F. Costanza, C. Diez Pardos, G. Dolinska,

G. Eckerlin, D. Eckstein, E. Gallo¹⁹, J. Garay Garcia, A. Geiser, A. Gizhko, J.M. Grados Luyando, P. Gunnellini, A. Harb, J. Hauk, M. Hempel²⁰, H. Jung, A. Kalogeropoulos, O. Karacheban²⁰, M. Kasemann, J. Keaveney, J. Kieseler, C. Kleinwort, I. Korol, W. Lange, A. Lelek, J. Leonard, K. Lipka, A. Lobanov, W. Lohmann²⁰, R. Mankel, I.-A. Melzer-Pellmann, A.B. Meyer, G. Mittag, J. Mnich, A. Mussgiller, E. Ntomari, D. Pitzl, R. Placakyte, A. Raspereza, B. Roland, M.Ö. Sahin, P. Saxena, T. Schoerner-Sadenius, C. Seitz, S. Spannagel, N. Stefaniuk, K.D. Trippkewitz, G.P. Van Onsem, R. Walsh, C. Wissing

University of Hamburg, Hamburg, Germany

V. Blobel, M. Centis Vignali, A.R. Draeger, T. Dreyer, E. Garutti, K. Goebel, D. Gonzalez, J. Haller, M. Hoffmann, R.S. Höing, A. Junkes, R. Klanner, R. Kogler, N. Kovalchuk, T. Lapsien, T. Lenz, I. Marchesini, D. Marconi, M. Meyer, M. Niedziela, D. Nowatschin, J. Ott, F. Pantaleo¹⁵, T. Peiffer, A. Perieanu, J. Poehlsen, C. Sander, C. Scharf, P. Schleper, E. Schlieckau, A. Schmidt, S. Schumann, J. Schwandt, H. Stadie, G. Steinbrück, F.M. Stober, M. Stöver, H. Tholen, D. Troendle, E. Usai, L. Vanelderren, A. Vanhoefer, B. Vormwald

Institut für Experimentelle Kernphysik, Karlsruhe, Germany

C. Barth, C. Baus, J. Berger, E. Butz, T. Chwalek, F. Colombo, W. De Boer, A. Dierlamm, S. Fink, R. Friese, M. Giffels, A. Gilbert, D. Haitz, F. Hartmann¹⁵, S.M. Heindl, U. Husemann, I. Katkov¹⁶, A. Kornmayer¹⁵, P. Lobelle Pardo, B. Maier, H. Mildner, M.U. Mozer, T. Müller, Th. Müller, M. Plagge, G. Quast, K. Rabbertz, S. Röcker, F. Roscher, M. Schröder, G. Sieber, H.J. Simonis, R. Ulrich, J. Wagner-Kuhr, S. Wayand, M. Weber, T. Weiler, S. Williamson, C. Wöhrmann, R. Wolf

Institute of Nuclear and Particle Physics (INPP), NCSR Demokritos, Aghia Paraskevi, Greece

G. Anagnostou, G. Daskalakis, T. Gerasis, V.A. Giakoumopoulou, A. Kyriakis, D. Loukas, I. Topsis-Giotis

National and Kapodistrian University of Athens, Athens, Greece

A. Agapitos, S. Kesisoglou, A. Panagiotou, N. Saoulidou, E. Tziaferi

University of Ioánnina, Ioánnina, Greece

I. Evangelou, G. Flouris, C. Foudas, P. Kokkas, N. Loukas, N. Manthos, I. Papadopoulos, E. Paradas

MTA-ELTE Lendület CMS Particle and Nuclear Physics Group, Eötvös Loránd University, Budapest, Hungary

N. Filipovic

Wigner Research Centre for Physics, Budapest, Hungary

G. Bencze, C. Hajdu, P. Hidas, D. Horvath²¹, F. Sikler, V. Veszpremi, G. Vesztergombi²², A.J. Zsigmond

Institute of Nuclear Research ATOMKI, Debrecen, Hungary

N. Beni, S. Czellar, J. Karancsi²³, J. Molnar, Z. Szillasi

University of Debrecen, Debrecen, Hungary

M. Bartók²², A. Makovec, P. Raics, Z.L. Trocsanyi, B. Ujvari

National Institute of Science Education and Research, Bhubaneswar, India

S. Bahinipati, S. Choudhury²⁴, P. Mal, K. Mandal, A. Nayak²⁵, D.K. Sahoo, N. Sahoo, S.K. Swain

Panjab University, Chandigarh, India

S. Bansal, S.B. Beri, V. Bhatnagar, R. Chawla, R. Gupta, U. Bhawandeep, A.K. Kalsi, A. Kaur, M. Kaur, R. Kumar, A. Mehta, M. Mittal, J.B. Singh, G. Walia

University of Delhi, Delhi, India

Ashok Kumar, A. Bhardwaj, B.C. Choudhary, R.B. Garg, S. Keshri, A. Kumar, S. Malhotra, M. Naimuddin, N. Nishu, K. Ranjan, R. Sharma, V. Sharma

Saha Institute of Nuclear Physics, Kolkata, India

R. Bhattacharya, S. Bhattacharya, K. Chatterjee, S. Dey, S. Dutt, S. Dutta, S. Ghosh, N. Majumdar, A. Modak, K. Mondal, S. Mukhopadhyay, S. Nandan, A. Purohit, A. Roy, D. Roy, S. Roy Chowdhury, S. Sarkar, M. Sharan, S. Thakur

Indian Institute of Technology Madras, Madras, India

P.K. Behera

Bhabha Atomic Research Centre, Mumbai, India

R. Chudasama, D. Dutta, V. Jha, V. Kumar, A.K. Mohanty¹⁵, P.K. Netrakanti, L.M. Pant, P. Shukla, A. Topkar

Tata Institute of Fundamental Research-A, Mumbai, India

T. Aziz, S. Dugad, G. Kole, B. Mahakud, S. Mitra, G.B. Mohanty, N. Sur, B. Sutar

Tata Institute of Fundamental Research-B, Mumbai, India

S. Banerjee, M. Guchait, Sa. Jain, G. Majumder, K. Mazumdar, N. Wickramage²⁶

Indian Institute of Science Education and Research (IISER), Pune, India

S. Chauhan, S. Dube, A. Kapoor, K. Kotheekar, A. Rane, S. Sharma

Institute for Research in Fundamental Sciences (IPM), Tehran, Iran

H. Bakhshiansohi, H. Behnamian, S. Chenarani²⁷, E. Eskandari Tadavani, S.M. Etesami²⁷, A. Fahim²⁸, M. Khakzad, M. Mohammadi Najafabadi, M. Naseri, S. Paktinat Mehdiabadi, F. Rezaei Hosseinabadi, B. Safarzadeh²⁹, M. Zeinali

University College Dublin, Dublin, Ireland

M. Felcini, M. Grunewald

INFN Sezione di Bari ^a, Università di Bari ^b, Politecnico di Bari ^c, Bari, Italy

M. Abbrescia^{a,b}, C. Calabria^{a,b}, C. Caputo^{a,b}, A. Colaleo^a, D. Creanza^{a,c}, L. Cristella^{a,b}, N. De Filippis^{a,c}, M. De Palma^{a,b}, L. Fiore^a, G. Iaselli^{a,c}, G. Maggi^{a,c}, M. Maggi^a, G. Miniello^{a,b}, S. My^{a,b}, S. Nuzzo^{a,b}, A. Pompili^{a,b}, G. Pugliese^{a,c}, R. Radogna^{a,b}, A. Ranieri^a, G. Selvaggi^{a,b}, L. Silvestris^{a,15}, R. Venditti^{a,b}

INFN Sezione di Bologna ^a, Università di Bologna ^b, Bologna, Italy

G. Abbiendi^a, C. Battilana, D. Bonacorsi^{a,b}, S. Braibant-Giacomelli^{a,b}, L. Brigliadori^{a,b}, R. Campanini^{a,b}, P. Capiluppi^{a,b}, A. Castro^{a,b}, F.R. Cavallo^a, S.S. Chhibra^{a,b}, G. Codispoti^{a,b}, M. Cuffiani^{a,b}, G.M. Dallavalle^a, F. Fabbri^a, A. Fanfani^{a,b}, D. Fasanella^{a,b}, P. Giacomelli^a, C. Grandi^a, L. Guiducci^{a,b}, S. Marcellini^a, G. Masetti^a, A. Montanari^a, F.L. Navarria^{a,b}, A. Perrotta^a, A.M. Rossi^{a,b}, T. Rovelli^{a,b}, G.P. Siroli^{a,b}, N. Tosi^{a,b,15}

INFN Sezione di Catania ^a, Università di Catania ^b, Catania, Italy

S. Albergo^{a,b}, M. Chiorboli^{a,b}, S. Costa^{a,b}, A. Di Mattia^a, F. Giordano^{a,b}, R. Potenza^{a,b}, A. Tricomi^{a,b}, C. Tuve^{a,b}

INFN Sezione di Firenze ^a, Università di Firenze ^b, Firenze, Italy

G. Barbagli^a, V. Ciulli^{a,b}, C. Civinini^a, R. D'Alessandro^{a,b}, E. Focardi^{a,b}, V. Gori^{a,b}, P. Lenzi^{a,b}, M. Meschini^a, S. Paoletti^a, G. Sguazzoni^a, L. Viliani^{a,b,15}

INFN Laboratori Nazionali di Frascati, Frascati, Italy

L. Benussi, S. Bianco, F. Fabbri, D. Piccolo, F. Primavera¹⁵

INFN Sezione di Genova ^a, Università di Genova ^b, Genova, Italy

V. Calvelli^{a,b}, F. Ferro^a, M. Lo Vetere^{a,b}, M.R. Monge^{a,b}, E. Robutti^a, S. Tosi^{a,b}

INFN Sezione di Milano-Bicocca ^a, Università di Milano-Bicocca ^b, Milano, Italy

L. Brianza, M.E. Dinardo^{a,b}, S. Fiorendi^{a,b}, S. Gennai^a, A. Ghezzi^{a,b}, P. Govoni^{a,b}, S. Malvezzi^a, R.A. Manzoni^{a,b,15}, B. Marzocchi^{a,b}, D. Menasce^a, L. Moroni^a, M. Paganoni^{a,b}, D. Pedrini^a, S. Pigazzini, S. Ragazzi^{a,b}, T. Tabarelli de Fatis^{a,b}

INFN Sezione di Napoli ^a, Università di Napoli 'Federico II' ^b, Napoli, Italy, Università della Basilicata ^c, Potenza, Italy, Università G. Marconi ^d, Roma, Italy

S. Buontempo^a, N. Cavallo^{a,c}, G. De Nardo, S. Di Guida^{a,d,15}, M. Esposito^{a,b}, F. Fabozzi^{a,c}, A.O.M. Iorio^{a,b}, G. Lanza^a, L. Lista^a, S. Meola^{a,d,15}, M. Merola^a, P. Paolucci^{a,15}, C. Sciacca^{a,b}, F. Thyssen

INFN Sezione di Padova ^a, Università di Padova ^b, Padova, Italy, Università di Trento ^c, Trento, Italy

P. Azzi^{a,15}, N. Bacchetta^a, L. Benato^{a,b}, D. Bisello^{a,b}, A. Boletti^{a,b}, R. Carlin^{a,b}, A. Carvalho Antunes De Oliveira^{a,b}, P. Checchia^a, M. Dall'Osso^{a,b}, P. De Castro Manzano^a, T. Dorigo^a, U. Dosselli^a, F. Gasparini^{a,b}, U. Gasparini^{a,b}, A. Gozzelino^a, S. Lacaprara^a, M. Margoni^{a,b}, A.T. Meneguzzo^{a,b}, J. Pazzini^{a,b,15}, N. Pozzobon^{a,b}, P. Ronchese^{a,b}, F. Simonetto^{a,b}, E. Torassa^a, M. Zanetti, P. Zotto^{a,b}, A. Zucchetta^{a,b}, G. Zumerle^{a,b}

INFN Sezione di Pavia ^a, Università di Pavia ^b, Pavia, Italy

A. Braghieri^a, A. Magnani^{a,b}, P. Montagna^{a,b}, S.P. Ratti^{a,b}, V. Re^a, C. Riccardi^{a,b}, P. Salvini^a, I. Vai^{a,b}, P. Vitulo^{a,b}

INFN Sezione di Perugia ^a, Università di Perugia ^b, Perugia, Italy

L. Alunni Solestizi^{a,b}, G.M. Bilei^a, D. Ciangottini^{a,b}, L. Fanò^{a,b}, P. Lariccia^{a,b}, R. Leonardi^{a,b}, G. Mantovani^{a,b}, M. Menichelli^a, A. Saha^a, A. Santocchia^{a,b}

INFN Sezione di Pisa ^a, Università di Pisa ^b, Scuola Normale Superiore di Pisa ^c, Pisa, Italy

K. Androsov^{a,30}, P. Azzurri^{a,15}, G. Bagliesi^a, J. Bernardini^a, T. Boccali^a, R. Castaldi^a, M.A. Ciocci^{a,30}, R. Dell'Orso^a, S. Donato^{a,c}, G. Fedi, A. Giassi^a, M.T. Grippo^{a,30}, F. Ligabue^{a,c}, T. Lomtadze^a, L. Martini^{a,b}, A. Messineo^{a,b}, F. Palla^a, A. Rizzi^{a,b}, A. Savoy-Navarro^{a,31}, P. Spagnolo^a, R. Tenchini^a, G. Tonelli^{a,b}, A. Venturi^a, P.G. Verdini^a

INFN Sezione di Roma ^a, Università di Roma ^b, Roma, Italy

L. Barone^{a,b}, F. Cavallari^a, M. Cipriani^{a,b}, G. D'imperio^{a,b,15}, D. Del Re^{a,b,15}, M. Diemoz^a, S. Gelli^{a,b}, C. Jordà^a, E. Longo^{a,b}, F. Margaroli^{a,b}, P. Meridiani^a, G. Organtini^{a,b}, R. Paramatti^a, F. Preiato^{a,b}, S. Rahatlou^{a,b}, C. Rovelli^a, F. Santanastasio^{a,b}

INFN Sezione di Torino ^a, Università di Torino ^b, Torino, Italy, Università del Piemonte Orientale ^c, Novara, Italy

N. Amapane^{a,b}, R. Arcidiacono^{a,c,15}, S. Argiro^{a,b}, M. Arneodo^{a,c}, N. Bartosik^a, R. Bellan^{a,b}, C. Biino^a, N. Cartiglia^a, M. Costa^{a,b}, R. Covarelli^{a,b}, A. Degano^{a,b}, N. Demaria^a, L. Finco^{a,b}, B. Kiani^{a,b}, C. Mariotti^a, S. Maselli^a, E. Migliore^{a,b}, V. Monaco^{a,b}, E. Monteil^{a,b}, M.M. Obertino^{a,b}, L. Pacher^{a,b}, N. Pastrone^a, M. Pelliccioni^a, G.L. Pinna Angioni^{a,b}, F. Ravera^{a,b}

A. Romero^{a,b}, M. Ruspa^{a,c}, R. Sacchi^{a,b}, K. Shchelina^{a,b}, V. Sola^a, A. Solano^{a,b}, A. Staiano^a, P. Traczyk^{a,b}

INFN Sezione di Trieste ^a, Università di Trieste ^b, Trieste, Italy

S. Belforte^a, V. Candelise^{a,b}, M. Casarsa^a, F. Cossutti^a, G. Della Ricca^{a,b}, C. La Licata^{a,b}, A. Schizzi^{a,b}, A. Zanetti^a

Kyungpook National University, Daegu, Korea

D.H. Kim, G.N. Kim, M.S. Kim, S. Lee, S.W. Lee, Y.D. Oh, S. Sekmen, D.C. Son, Y.C. Yang

Chonbuk National University, Jeonju, Korea

H. Kim, A. Lee

Hanyang University, Seoul, Korea

J.A. Brochero Cifuentes, T.J. Kim

Korea University, Seoul, Korea

S. Cho, S. Choi, Y. Go, D. Gyun, S. Ha, B. Hong, Y. Jo, Y. Kim, B. Lee, K. Lee, K.S. Lee, S. Lee, J. Lim, S.K. Park, Y. Roh

Seoul National University, Seoul, Korea

J. Almond, J. Kim, S.B. Oh, S.h. Seo, U.K. Yang, H.D. Yoo, G.B. Yu

University of Seoul, Seoul, Korea

M. Choi, H. Kim, H. Kim, J.H. Kim, J.S.H. Lee, I.C. Park, G. Ryu, M.S. Ryu

Sungkyunkwan University, Suwon, Korea

Y. Choi, J. Goh, D. Kim, E. Kwon, J. Lee, I. Yu

Vilnius University, Vilnius, Lithuania

V. Dudenas, A. Juodagalvis, J. Vaitkus

National Centre for Particle Physics, Universiti Malaya, Kuala Lumpur, Malaysia

I. Ahmed, Z.A. Ibrahim, J.R. Komaragiri, M.A.B. Md Ali³², F. Mohamad Idris³³, W.A.T. Wan Abdullah, M.N. Yusli, Z. Zolkapli

Centro de Investigacion y de Estudios Avanzados del IPN, Mexico City, Mexico

H. Castilla-Valdez, E. De La Cruz-Burelo, I. Heredia-De La Cruz³⁴, A. Hernandez-Almada, R. Lopez-Fernandez, J. Mejia Guisao, A. Sanchez-Hernandez

Universidad Iberoamericana, Mexico City, Mexico

S. Carrillo Moreno, F. Vazquez Valencia

Benemerita Universidad Autonoma de Puebla, Puebla, Mexico

S. Carpinteyro, I. Pedraza, H.A. Salazar Ibarquen, C. Uribe Estrada

Universidad Autónoma de San Luis Potosí, San Luis Potosí, Mexico

A. Morelos Pineda

University of Auckland, Auckland, New Zealand

D. Krofcheck

University of Canterbury, Christchurch, New Zealand

P.H. Butler

National Centre for Physics, Quaid-I-Azam University, Islamabad, Pakistan

A. Ahmad, M. Ahmad, Q. Hassan, H.R. Hoorani, W.A. Khan, M.A. Shah, M. Shoaib, M. Waqas

National Centre for Nuclear Research, Swierk, Poland

H. Bialkowska, M. Bluj, B. Boimska, T. Frueboes, M. Górski, M. Kazana, K. Nawrocki, K. Romanowska-Rybinska, M. Szleper, P. Zalewski

Institute of Experimental Physics, Faculty of Physics, University of Warsaw, Warsaw, Poland

K. Bunkowski, A. Byszuk³⁵, K. Doroba, A. Kalinowski, M. Konecki, J. Krolikowski, M. Misiura, M. Olszewski, M. Walczak

Laboratório de Instrumentação e Física Experimental de Partículas, Lisboa, Portugal

P. Bargassa, C. Beirão Da Cruz E Silva, A. Di Francesco, P. Faccioli, P.G. Ferreira Parracho, M. Gallinaro, J. Hollar, N. Leonardo, L. Lloret Iglesias, M.V. Nemallapudi, J. Rodrigues Antunes, J. Seixas, O. Toldaiev, D. Vadrucchio, J. Varela, P. Vischia

Joint Institute for Nuclear Research, Dubna, Russia

P. Bunin, A. Golunov, I. Golutvin, N. Gorbounov, V. Karjavin, V. Korenkov, A. Lanev, A. Malakhov, V. Matveev^{36,37}, V.V. Mitsyn, P. Moisenz, V. Palichik, V. Perelygin, S. Shmatov, S. Shulha, N. Skatchkov, V. Smirnov, E. Tikhonenko, A. Zarubin

Petersburg Nuclear Physics Institute, Gatchina (St. Petersburg), Russia

L. Chtchypounov, V. Golovtsov, Y. Ivanov, V. Kim³⁸, E. Kuznetsova³⁹, V. Murzin, V. Oreshkin, V. Sulimov, A. Vorobyev

Institute for Nuclear Research, Moscow, Russia

Yu. Andreev, A. Dermenev, S. Gninenko, N. Golubev, A. Karneyeu, M. Kirsanov, N. Krasnikov, A. Pashenkov, D. Tlisov, A. Toropin

Institute for Theoretical and Experimental Physics, Moscow, Russia

V. Epshteyn, V. Gavrilov, N. Lychkovskaya, V. Popov, I. Pozdnyakov, G. Safronov, A. Spiridonov, M. Toms, E. Vlasov, A. Zhokin

National Research Nuclear University 'Moscow Engineering Physics Institute' (MEPhI), Moscow, Russia

R. Chistov⁴⁰, V. Rusinov, E. Tarkovskii

P.N. Lebedev Physical Institute, Moscow, Russia

V. Andreev, M. Azarkin³⁷, I. Dremin³⁷, M. Kirakosyan, A. Leonidov³⁷, S.V. Rusakov, A. Terkulov

Skobeltsyn Institute of Nuclear Physics, Lomonosov Moscow State University, Moscow, Russia

A. Baskakov, A. Belyaev, E. Boos, V. Bunichev, M. Dubinin⁴¹, L. Dudko, A. Ershov, V. Klyukhin, O. Kodolova, N. Korneeva, I. Lokhtin, I. Miagkov, S. Obraztsov, M. Perfilov, V. Savrin

State Research Center of Russian Federation, Institute for High Energy Physics, Protvino, Russia

I. Azhgirey, I. Bayshev, S. Bitioukov, D. Elumakhov, V. Kachanov, A. Kalinin, D. Konstantinov, V. Krychkine, V. Petrov, R. Ryutin, A. Sobol, S. Troshin, N. Tyurin, A. Uzunian, A. Volkov

University of Belgrade, Faculty of Physics and Vinca Institute of Nuclear Sciences, Belgrade, Serbia

P. Adzic⁴², P. Cirkovic, D. Devetak, J. Milosevic, V. Rekovic

Centro de Investigaciones Energéticas Medioambientales y Tecnológicas (CIEMAT), Madrid, Spain

J. Alcaraz Maestre, E. Calvo, M. Cerrada, M. Chamizo Llatas, N. Colino, B. De La Cruz,

A. Delgado Peris, A. Escalante Del Valle, C. Fernandez Bedoya, J.P. Fernández Ramos, J. Flix, M.C. Fouz, P. Garcia-Abia, O. Gonzalez Lopez, S. Goy Lopez, J.M. Hernandez, M.I. Josa, E. Navarro De Martino, A. Pérez-Calero Yzquierdo, J. Puerta Pelayo, A. Quintario Olmeda, I. Redondo, L. Romero, M.S. Soares

Universidad Autónoma de Madrid, Madrid, Spain

J.F. de Trocóniz, M. Missiroli, D. Moran

Universidad de Oviedo, Oviedo, Spain

J. Cuevas, J. Fernandez Menendez, I. Gonzalez Caballero, J.R. González Fernández, E. Palencia Cortezon, S. Sanchez Cruz, J.M. Vizán Garcia

Instituto de Física de Cantabria (IFCA), CSIC-Universidad de Cantabria, Santander, Spain

I.J. Cabrillo, A. Calderon, J.R. Castiñeiras De Saa, E. Curras, M. Fernandez, J. Garcia-Ferrero, G. Gomez, A. Lopez Virto, J. Marco, C. Martinez Rivero, F. Matorras, J. Piedra Gomez, T. Rodrigo, A. Ruiz-Jimeno, L. Scodellaro, N. Trevisani, I. Vila, R. Vilar Cortabitarte

CERN, European Organization for Nuclear Research, Geneva, Switzerland

D. Abbaneo, E. Auffray, G. Auzinger, M. Bachtis, P. Baillon, A.H. Ball, D. Barney, P. Bloch, A. Bocci, A. Bonato, C. Botta, T. Camporesi, R. Castello, M. Cepeda, G. Cerminara, M. D'Alfonso, D. d'Enterria, A. Dabrowski, V. Daponte, A. David, M. De Gruttola, F. De Guio, A. De Roeck, E. Di Marco⁴³, M. Dobson, M. Dordevic, B. Dorney, T. du Pree, D. Duggan, M. Dünser, N. Dupont, A. Elliott-Peisert, S. Fartoukh, G. Franzoni, J. Fulcher, W. Funk, D. Gigi, K. Gill, M. Girone, F. Glege, S. Gundacker, M. Guthoff, J. Hammer, P. Harris, J. Hegeman, V. Innocente, P. Janot, H. Kirschenmann, V. Knünz, M.J. Kortelainen, K. Kousouris, M. Kramer¹, P. Lecoq, C. Lourenço, M.T. Lucchini, L. Malgeri, M. Mannelli, A. Martelli, F. Meijers, S. Mersi, E. Meschi, F. Moortgat, S. Morovic, M. Mulders, H. Neugebauer, S. Orfanelli⁴⁴, L. Orsini, L. Pape, E. Perez, M. Peruzzi, A. Petrilli, G. Petrucciani, A. Pfeiffer, M. Pierini, A. Racz, T. Reis, G. Rolandi⁴⁵, M. Rovere, M. Ruan, H. Sakulin, J.B. Sauvan, C. Schäfer, C. Schwick, M. Seidel, A. Sharma, P. Silva, M. Simon, P. Sphicas⁴⁶, J. Steggemann, M. Stoye, Y. Takahashi, M. Tosi, D. Treille, A. Triossi, A. Tsirou, V. Veckalns⁴⁷, G.I. Veres²², N. Wardle, H.K. Wöhri, A. Zagozdinska³⁵, W.D. Zeuner

Paul Scherrer Institut, Villigen, Switzerland

W. Bertl, K. Deiters, W. Erdmann, R. Horisberger, Q. Ingram, H.C. Kaestli, D. Kotlinski, U. Langenegger, T. Rohe

Institute for Particle Physics, ETH Zurich, Zurich, Switzerland

F. Bachmair, L. Bäni, L. Bianchini, B. Casal, G. Dissertori, M. Dittmar, M. Donegà, P. Eller, C. Grab, C. Heidegger, D. Hits, J. Hoss, G. Kasieczka, P. Lecomte[†], W. Lustermann, B. Mangano, M. Marionneau, P. Martinez Ruiz del Arbol, M. Masciovecchio, M.T. Meinhard, D. Meister, F. Micheli, P. Musella, F. Nessi-Tedaldi, F. Pandolfi, J. Pata, F. Pauss, G. Perrin, L. Perrozzi, M. Quittnat, M. Rossini, M. Schönenberger, A. Starodumov⁴⁸, M. Takahashi, V.R. Tavolaro, K. Theofilatos, R. Wallny

Universität Zürich, Zurich, Switzerland

T.K. Aarrestad, C. AMSler⁴⁹, L. Caminada, M.F. Canelli, V. Chiochia, A. De Cosa, C. Galloni, A. Hinzmann, T. Hreus, B. Kilminster, C. Lange, J. Ngadiuba, D. Pinna, G. Rauco, P. Robmann, D. Salerno, Y. Yang

National Central University, Chung-Li, Taiwan

T.H. Doan, Sh. Jain, R. Khurana, M. Konyushikhin, C.M. Kuo, W. Lin, Y.J. Lu, A. Pozdnyakov, S.S. Yu

National Taiwan University (NTU), Taipei, Taiwan

Arun Kumar, P. Chang, Y.H. Chang, Y.W. Chang, Y. Chao, K.F. Chen, P.H. Chen, C. Dietz, F. Fiori, W.-S. Hou, Y. Hsiung, Y.F. Liu, R.-S. Lu, M. Miñano Moya, E. Paganis, A. Psallidas, J.f. Tsai, Y.M. Tzeng

Chulalongkorn University, Faculty of Science, Department of Physics, Bangkok, Thailand

B. Asavapibhop, G. Singh, N. Srimanobhas, N. Suwonjandee

Cukurova University, Adana, Turkey

A. Adiguzel, S. Cerci⁵⁰, S. Damarseckin, Z.S. Demiroglu, C. Dozen, I. Dumanoglu, S. Girgis, G. Gokbulut, Y. Guler, E. Gurpinar, I. Hos, E.E. Kangal⁵¹, G. Onengut⁵², K. Ozdemir⁵³, D. Sunar Cerci⁵⁰, B. Tali⁵⁰, H. Topakli⁵⁴, S. Turkcapar, C. Zorbilmez

Middle East Technical University, Physics Department, Ankara, Turkey

B. Bilin, S. Bilmis, B. Isildak⁵⁵, G. Karapinar⁵⁶, M. Yalvac, M. Zeyrek

Bogazici University, Istanbul, Turkey

E. Gülmez, M. Kaya⁵⁷, O. Kaya⁵⁸, E.A. Yetkin⁵⁹, T. Yetkin⁶⁰

Istanbul Technical University, Istanbul, Turkey

A. Cakir, K. Cankocak, S. Sen⁶¹

Institute for Scintillation Materials of National Academy of Science of Ukraine, Kharkov, Ukraine

B. Grynyov

National Scientific Center, Kharkov Institute of Physics and Technology, Kharkov, Ukraine

L. Levchuk, P. Sorokin

University of Bristol, Bristol, United Kingdom

R. Aggleton, F. Ball, L. Beck, J.J. Brooke, D. Burns, E. Clement, D. Cussans, H. Flacher, J. Goldstein, M. Grimes, G.P. Heath, H.F. Heath, J. Jacob, L. Kreczko, C. Lucas, D.M. Newbold⁶², S. Paramesvaran, A. Poll, T. Sakuma, S. Seif El Nasr-storey, D. Smith, V.J. Smith

Rutherford Appleton Laboratory, Didcot, United Kingdom

K.W. Bell, A. Belyaev⁶³, C. Brew, R.M. Brown, L. Calligaris, D. Cieri, D.J.A. Cockerill, J.A. Coughlan, K. Harder, S. Harper, E. Olaiya, D. Petyt, C.H. Shepherd-Themistocleous, A. Thea, I.R. Tomalin, T. Williams

Imperial College, London, United Kingdom

M. Baber, R. Bainbridge, O. Buchmuller, A. Bundock, D. Burton, S. Casasso, M. Citron, D. Colling, L. Corpe, P. Dauncey, G. Davies, A. De Wit, M. Della Negra, P. Dunne, A. Elwood, D. Futyan, Y. Haddad, G. Hall, G. Iles, R. Lane, C. Laner, R. Lucas⁶², L. Lyons, A.-M. Magnan, S. Malik, L. Mastrolorenzo, J. Nash, A. Nikitenko⁴⁸, J. Pela, B. Penning, M. Pesaresi, D.M. Raymond, A. Richards, A. Rose, C. Seez, A. Tapper, K. Uchida, M. Vazquez Acosta⁶⁴, T. Virdee¹⁵, S.C. Zenz

Brunel University, Uxbridge, United Kingdom

J.E. Cole, P.R. Hobson, A. Khan, P. Kyberd, D. Leslie, I.D. Reid, P. Symonds, L. Teodorescu, M. Turner

Baylor University, Waco, USA

A. Borzou, K. Call, J. Dittmann, K. Hatakeyama, H. Liu, N. Pastika

The University of Alabama, Tuscaloosa, USA

O. Charaf, S.I. Cooper, C. Henderson, P. Rumerio

Boston University, Boston, USA

D. Arcaro, A. Avetisyan, T. Bose, D. Gastler, D. Rankin, C. Richardson, J. Rohlf, L. Sulak, D. Zou

Brown University, Providence, USA

G. Benelli, E. Berry, D. Cutts, A. Ferapontov, A. Garabedian, J. Hakala, U. Heintz, O. Jesus, E. Laird, G. Landsberg, Z. Mao, M. Narain, S. Piperov, S. Sagir, E. Spencer, R. Syarif

University of California, Davis, Davis, USA

R. Breedon, G. Breto, D. Burns, M. Calderon De La Barca Sanchez, S. Chauhan, M. Chertok, J. Conway, R. Conway, P.T. Cox, R. Erbacher, C. Flores, G. Funk, M. Gardner, W. Ko, R. Lander, C. Mclean, M. Mulhearn, D. Pellett, J. Pilot, F. Ricci-Tam, S. Shalhout, J. Smith, M. Squires, D. Stolp, M. Tripathi, S. Wilbur, R. Yohay

University of California, Los Angeles, USA

R. Cousins, P. Everaerts, A. Florent, J. Hauser, M. Ignatenko, D. Saltzberg, E. Takasugi, V. Valuev, M. Weber

University of California, Riverside, Riverside, USA

K. Burt, R. Clare, J. Ellison, J.W. Gary, G. Hanson, J. Heilman, P. Jandir, E. Kennedy, F. Lacroix, O.R. Long, M. Malberti, M. Olmedo Negrete, M.I. Paneva, A. Shrinivas, H. Wei, S. Wimpenny, B. R. Yates

University of California, San Diego, La Jolla, USA

J.G. Branson, G.B. Cerati, S. Cittolin, M. Derdzinski, R. Gerosa, A. Holzner, D. Klein, J. Letts, I. Macneill, D. Olivito, S. Padhi, M. Pieri, M. Sani, V. Sharma, S. Simon, M. Tadel, A. Vartak, S. Wasserbaech⁶⁵, C. Welke, J. Wood, F. Würthwein, A. Yagil, G. Zevi Della Porta

University of California, Santa Barbara - Department of Physics, Santa Barbara, USA

R. Bhandari, J. Bradmiller-Feld, C. Campagnari, A. Dishaw, V. Dutta, K. Flowers, M. Franco Sevilla, P. Geffert, C. George, F. Golf, L. Gouskos, J. Gran, R. Heller, J. Incandela, N. Mccoll, S.D. Mullin, A. Ovcharova, J. Richman, D. Stuart, I. Suarez, C. West, J. Yoo

California Institute of Technology, Pasadena, USA

D. Anderson, A. Apresyan, J. Bendavid, A. Bornheim, J. Bunn, Y. Chen, J. Duarte, A. Mott, H.B. Newman, C. Pena, M. Spiropulu, J.R. Vlimant, S. Xie, R.Y. Zhu

Carnegie Mellon University, Pittsburgh, USA

M.B. Andrews, V. Azzolini, A. Calamba, B. Carlson, T. Ferguson, M. Paulini, J. Russ, M. Sun, H. Vogel, I. Vorobiev

University of Colorado Boulder, Boulder, USA

J.P. Cumalat, W.T. Ford, F. Jensen, A. Johnson, M. Krohn, T. Mulholland, K. Stenson, S.R. Wagner

Cornell University, Ithaca, USA

J. Alexander, J. Chaves, J. Chu, S. Dittmer, N. Mirman, G. Nicolas Kaufman, J.R. Patterson, A. Rinkevicius, A. Ryd, L. Skinnari, W. Sun, S.M. Tan, Z. Tao, J. Thom, J. Tucker, P. Wittich

Fairfield University, Fairfield, USA

D. Winn

Fermi National Accelerator Laboratory, Batavia, USA

S. Abdullin, M. Albrow, G. Apollinari, S. Banerjee, L.A.T. Bauerdick, A. Beretvas, J. Berryhill, P.C. Bhat, G. Bolla, K. Burkett, J.N. Butler, H.W.K. Cheung, F. Chlebana, S. Cihangir, M. Cremonesi, V.D. Elvira, I. Fisk, J. Freeman, E. Gottschalk, L. Gray, D. Green, S. Grünendahl,

O. Gutsche, D. Hare, R.M. Harris, S. Hasegawa, J. Hirschauer, Z. Hu, B. Jayatilaka, S. Jindariani, M. Johnson, U. Joshi, B. Klima, B. Kreis, S. Lammel, J. Linacre, D. Lincoln, R. Lipton, T. Liu, R. Lopes De Sá, J. Lykken, K. Maeshima, N. Magini, J.M. Marraffino, S. Maruyama, D. Mason, P. McBride, P. Merkel, S. Mrenna, S. Nahn, C. Newman-Holmes[†], V. O'Dell, K. Pedro, O. Prokofyev, G. Rakness, L. Ristori, E. Sexton-Kennedy, A. Soha, W.J. Spalding, L. Spiegel, S. Stoynev, N. Strobbe, L. Taylor, S. Tkaczyk, N.V. Tran, L. Uplegger, E.W. Vaandering, C. Vernieri, M. Verzocchi, R. Vidal, M. Wang, H.A. Weber, A. Whitbeck

University of Florida, Gainesville, USA

D. Acosta, P. Avery, P. Bortignon, D. Bourilkov, A. Brinkerhoff, A. Carnes, M. Carver, D. Curry, S. Das, R.D. Field, I.K. Furic, J. Konigsberg, A. Korytov, P. Ma, K. Matchev, H. Mei, P. Milenovic⁶⁶, G. Mitselmakher, D. Rank, L. Shchutska, D. Sperka, L. Thomas, J. Wang, S. Wang, J. Yelton

Florida International University, Miami, USA

S. Linn, P. Markowitz, G. Martinez, J.L. Rodriguez

Florida State University, Tallahassee, USA

A. Ackert, J.R. Adams, T. Adams, A. Askew, S. Bein, B. Diamond, S. Hagopian, V. Hagopian, K.F. Johnson, A. Khatiwada, H. Prosper, A. Santra, M. Weinberg

Florida Institute of Technology, Melbourne, USA

M.M. Baarmand, V. Bhopatkar, S. Colafranceschi⁶⁷, M. Hohlmann, D. Noonan, T. Roy, F. Yumiceva

University of Illinois at Chicago (UIC), Chicago, USA

M.R. Adams, L. Apanasevich, D. Berry, R.R. Betts, I. Bucinskaite, R. Cavanaugh, O. Evdokimov, L. Gauthier, C.E. Gerber, D.J. Hofman, P. Kurt, C. O'Brien, I.D. Sandoval Gonzalez, P. Turner, N. Varelas, Z. Wu, M. Zakaria, J. Zhang

The University of Iowa, Iowa City, USA

B. Bilki⁶⁸, W. Clarida, K. Dilsiz, S. Durgut, R.P. Gandrajula, M. Haytmyradov, V. Khristenko, J.-P. Merlo, H. Mermerkaya⁶⁹, A. Mestvirishvili, A. Moeller, J. Nachtman, H. Ogul, Y. Onel, F. Ozok⁷⁰, A. Penzo, C. Snyder, E. Tiras, J. Wetzel, K. Yi

Johns Hopkins University, Baltimore, USA

I. Anderson, B. Blumenfeld, A. Cocoros, N. Eminizer, D. Fehling, L. Feng, A.V. Gritsan, P. Maksimovic, M. Osherson, J. Roskes, U. Sarica, M. Swartz, M. Xiao, Y. Xin, C. You

The University of Kansas, Lawrence, USA

A. Al-bataineh, P. Baringer, A. Bean, J. Bowen, C. Bruner, J. Castle, R.P. Kenny III, A. Kropivnitskaya, D. Majumder, W. Mcbrayer, M. Murray, S. Sanders, R. Stringer, J.D. Tapia Takaki, Q. Wang

Kansas State University, Manhattan, USA

A. Ivanov, K. Kaadze, S. Khalil, M. Makouski, Y. Maravin, A. Mohammadi, L.K. Saini, N. Skhirtladze, S. Toda

Lawrence Livermore National Laboratory, Livermore, USA

D. Lange, F. Rebassoo, D. Wright

University of Maryland, College Park, USA

C. Anelli, A. Baden, O. Baron, A. Belloni, B. Calvert, S.C. Eno, C. Ferraioli, J.A. Gomez, N.J. Hadley, S. Jabeen, R.G. Kellogg, T. Kolberg, J. Kunkle, Y. Lu, A.C. Mignerey, Y.H. Shin, A. Skuja, M.B. Tonjes, S.C. Tonwar

Massachusetts Institute of Technology, Cambridge, USA

A. Apyan, R. Barbieri, A. Baty, R. Bi, K. Bierwagen, S. Brandt, W. Busza, I.A. Cali, Z. Demiragli, L. Di Matteo, G. Gomez Ceballos, M. Goncharov, D. Gulhan, D. Hsu, Y. Iiyama, G.M. Innocenti, M. Klute, D. Kovalskyi, K. Krajczar, Y.S. Lai, Y.-J. Lee, A. Levin, P.D. Luckey, A.C. Marini, C. Mcginn, C. Mironov, S. Narayanan, X. Niu, C. Paus, C. Roland, G. Roland, J. Salfeld-Nebgen, G.S.F. Stephans, K. Sumorok, K. Tatar, M. Varma, D. Velicanu, J. Veverka, J. Wang, T.W. Wang, B. Wyslouch, M. Yang, V. Zhukova

University of Minnesota, Minneapolis, USA

A.C. Benvenuti, R.M. Chatterjee, A. Evans, A. Finkel, A. Gude, P. Hansen, S. Kalafut, S.C. Kao, Y. Kubota, Z. Lesko, J. Mans, S. Nourbakhsh, N. Ruckstuhl, R. Rusack, N. Tambe, J. Turkewitz

University of Mississippi, Oxford, USA

J.G. Acosta, S. Oliveros

University of Nebraska-Lincoln, Lincoln, USA

E. Avdeeva, R. Bartek, K. Bloom, S. Bose, D.R. Claes, A. Dominguez, C. Fangmeier, R. Gonzalez Suarez, R. Kamalieddin, D. Knowlton, I. Kravchenko, F. Meier, J. Monroy, J.E. Siado, G.R. Snow, B. Stieger

State University of New York at Buffalo, Buffalo, USA

M. Alyari, J. Dolen, J. George, A. Godshalk, C. Harrington, I. Iashvili, J. Kaisen, A. Kharchilava, A. Kumar, A. Parker, S. Rappoccio, B. Roozbahani

Northeastern University, Boston, USA

G. Alverson, E. Barberis, D. Baumgartel, M. Chasco, A. Hortiangtham, A. Massironi, D.M. Morse, D. Nash, T. Orimoto, R. Teixeira De Lima, D. Trocino, R.-J. Wang, D. Wood

Northwestern University, Evanston, USA

S. Bhattacharya, K.A. Hahn, A. Kubik, J.F. Low, N. Mucia, N. Odell, B. Pollack, M.H. Schmitt, K. Sung, M. Trovato, M. Velasco

University of Notre Dame, Notre Dame, USA

N. Dev, M. Hildreth, K. Hurtado Anampa, C. Jessop, D.J. Karmgard, N. Kellams, K. Lannon, N. Marinelli, F. Meng, C. Mueller, Y. Musienko³⁶, M. Planer, A. Reinsvold, R. Ruchti, G. Smith, S. Taroni, N. Valls, M. Wayne, M. Wolf, A. Woodard

The Ohio State University, Columbus, USA

J. Alimena, L. Antonelli, J. Brinson, B. Bylsma, L.S. Durkin, S. Flowers, B. Francis, A. Hart, C. Hill, R. Hughes, W. Ji, B. Liu, W. Luo, D. Puigh, B.L. Winer, H.W. Wulsin

Princeton University, Princeton, USA

S. Cooperstein, O. Driga, P. Elmer, J. Hardenbrook, P. Hebda, J. Luo, D. Marlow, T. Medvedeva, M. Mooney, J. Olsen, C. Palmer, P. Piroué, D. Stickland, C. Tully, A. Zuranski

University of Puerto Rico, Mayaguez, USA

S. Malik

Purdue University, West Lafayette, USA

A. Barker, V.E. Barnes, D. Benedetti, S. Folgueras, L. Gutay, M.K. Jha, M. Jones, A.W. Jung, K. Jung, D.H. Miller, N. Neumeister, B.C. Radburn-Smith, X. Shi, J. Sun, A. Svyatkovskiy, F. Wang, W. Xie, L. Xu

Purdue University Calumet, Hammond, USA

N. Parashar, J. Stupak

Rice University, Houston, USA

A. Adair, B. Akgun, Z. Chen, K.M. Ecklund, F.J.M. Geurts, M. Guilbaud, W. Li, B. Michlin, M. Northup, B.P. Padley, R. Redjimi, J. Roberts, J. Rorie, Z. Tu, J. Zabel

University of Rochester, Rochester, USA

B. Betchart, A. Bodek, P. de Barbaro, R. Demina, Y.t. Duh, T. Ferbel, M. Galanti, A. Garcia-Bellido, J. Han, O. Hindrichs, A. Khukhunaishvili, K.H. Lo, P. Tan, M. Verzetti

Rutgers, The State University of New Jersey, Piscataway, USA

J.P. Chou, E. Contreras-Campana, Y. Gershtein, T.A. Gómez Espinosa, E. Halkiadakis, M. Heindl, D. Hidas, E. Hughes, S. Kaplan, R. Kunnawalkam Elayavalli, S. Kyriacou, A. Lath, K. Nash, H. Saka, S. Salur, S. Schnetzer, D. Sheffield, S. Somalwar, R. Stone, S. Thomas, P. Thomassen, M. Walker

University of Tennessee, Knoxville, USA

M. Foerster, J. Heideman, G. Riley, K. Rose, S. Spanier, K. Thapa

Texas A&M University, College Station, USA

O. Bouhali⁷¹, A. Castaneda Hernandez⁷¹, A. Celik, M. Dalchenko, M. De Mattia, A. Delgado, S. Dildick, R. Eusebi, J. Gilmore, T. Huang, E. Juska, T. Kamon⁷², V. Krutelyov, R. Mueller, Y. Pakhotin, R. Patel, A. Perloff, L. Perniè, D. Rathjens, A. Rose, A. Safonov, A. Tatarinov, K.A. Ulmer

Texas Tech University, Lubbock, USA

N. Akchurin, C. Cowden, J. Damgov, C. Dragoiu, P.R. Duderod, J. Faulkner, S. Kunori, K. Lamichhane, S.W. Lee, T. Libeiro, S. Undleeb, I. Volobouev, Z. Wang

Vanderbilt University, Nashville, USA

A.G. Delannoy, S. Greene, A. Gurrola, R. Janjam, W. Johns, C. Maguire, A. Melo, H. Ni, P. Sheldon, S. Tuo, J. Velkovska, Q. Xu

University of Virginia, Charlottesville, USA

M.W. Arenton, P. Barria, B. Cox, J. Goodell, R. Hirosky, A. Ledovskoy, H. Li, C. Neu, T. Sinthuprasith, X. Sun, Y. Wang, E. Wolfe, F. Xia

Wayne State University, Detroit, USA

C. Clarke, R. Harr, P.E. Karchin, P. Lamichhane, J. Sturdy

University of Wisconsin - Madison, Madison, WI, USA

D.A. Belknap, S. Dasu, L. Dodd, S. Duric, B. Gomber, M. Grothe, M. Herndon, A. Hervé, P. Klabbers, A. Lanaro, A. Levine, K. Long, R. Loveless, I. Ojalvo, T. Perry, G.A. Pierro, G. Polese, T. Ruggles, A. Savin, A. Sharma, N. Smith, W.H. Smith, D. Taylor, P. Verwilligen, N. Woods

Tata Institute of Fundamental Research, Mumbai, ZZ

S. Bhowmik⁷³, R.K. Dewanjee, S. Ganguly, S. Kumar, M. Maity⁷³, B. Parida, T. Sarkar⁷³

†: Deceased

1: Also at Vienna University of Technology, Vienna, Austria

2: Also at State Key Laboratory of Nuclear Physics and Technology, Peking University, Beijing, China

3: Also at Institut Pluridisciplinaire Hubert Curien, Université de Strasbourg, Université de Haute Alsace Mulhouse, CNRS/IN2P3, Strasbourg, France

4: Also at Universidade Estadual de Campinas, Campinas, Brazil

5: Also at Centre National de la Recherche Scientifique (CNRS) - IN2P3, Paris, France

- 6: Also at Université Libre de Bruxelles, Bruxelles, Belgium
- 7: Also at Deutsches Elektronen-Synchrotron, Hamburg, Germany
- 8: Also at Joint Institute for Nuclear Research, Dubna, Russia
- 9: Also at Helwan University, Cairo, Egypt
- 10: Now at Zewail City of Science and Technology, Zewail, Egypt
- 11: Also at Ain Shams University, Cairo, Egypt
- 12: Also at Fayoum University, El-Fayoum, Egypt
- 13: Now at British University in Egypt, Cairo, Egypt
- 14: Also at Université de Haute Alsace, Mulhouse, France
- 15: Also at CERN, European Organization for Nuclear Research, Geneva, Switzerland
- 16: Also at Skobeltsyn Institute of Nuclear Physics, Lomonosov Moscow State University, Moscow, Russia
- 17: Also at Tbilisi State University, Tbilisi, Georgia
- 18: Also at RWTH Aachen University, III. Physikalisches Institut A, Aachen, Germany
- 19: Also at University of Hamburg, Hamburg, Germany
- 20: Also at Brandenburg University of Technology, Cottbus, Germany
- 21: Also at Institute of Nuclear Research ATOMKI, Debrecen, Hungary
- 22: Also at MTA-ELTE Lendület CMS Particle and Nuclear Physics Group, Eötvös Loránd University, Budapest, Hungary
- 23: Also at University of Debrecen, Debrecen, Hungary
- 24: Also at Indian Institute of Science Education and Research, Bhopal, India
- 25: Also at Institute of Physics, Bhubaneswar, India
- 26: Also at University of Ruhuna, Matara, Sri Lanka
- 27: Also at Isfahan University of Technology, Isfahan, Iran
- 28: Also at University of Tehran, Department of Engineering Science, Tehran, Iran
- 29: Also at Plasma Physics Research Center, Science and Research Branch, Islamic Azad University, Tehran, Iran
- 30: Also at Università degli Studi di Siena, Siena, Italy
- 31: Also at Purdue University, West Lafayette, USA
- 32: Also at International Islamic University of Malaysia, Kuala Lumpur, Malaysia
- 33: Also at Malaysian Nuclear Agency, MOSTI, Kajang, Malaysia
- 34: Also at Consejo Nacional de Ciencia y Tecnología, Mexico city, Mexico
- 35: Also at Warsaw University of Technology, Institute of Electronic Systems, Warsaw, Poland
- 36: Also at Institute for Nuclear Research, Moscow, Russia
- 37: Now at National Research Nuclear University 'Moscow Engineering Physics Institute' (MEPhI), Moscow, Russia
- 38: Also at St. Petersburg State Polytechnical University, St. Petersburg, Russia
- 39: Also at University of Florida, Gainesville, USA
- 40: Also at P.N. Lebedev Physical Institute, Moscow, Russia
- 41: Also at California Institute of Technology, Pasadena, USA
- 42: Also at Faculty of Physics, University of Belgrade, Belgrade, Serbia
- 43: Also at INFN Sezione di Roma; Università di Roma, Roma, Italy
- 44: Also at National Technical University of Athens, Athens, Greece
- 45: Also at Scuola Normale e Sezione dell'INFN, Pisa, Italy
- 46: Also at National and Kapodistrian University of Athens, Athens, Greece
- 47: Also at Riga Technical University, Riga, Latvia
- 48: Also at Institute for Theoretical and Experimental Physics, Moscow, Russia
- 49: Also at Albert Einstein Center for Fundamental Physics, Bern, Switzerland
- 50: Also at Adiyaman University, Adiyaman, Turkey

-
- 51: Also at Mersin University, Mersin, Turkey
 - 52: Also at Cag University, Mersin, Turkey
 - 53: Also at Piri Reis University, Istanbul, Turkey
 - 54: Also at Gaziosmanpasa University, Tokat, Turkey
 - 55: Also at Ozyegin University, Istanbul, Turkey
 - 56: Also at Izmir Institute of Technology, Izmir, Turkey
 - 57: Also at Marmara University, Istanbul, Turkey
 - 58: Also at Kafkas University, Kars, Turkey
 - 59: Also at Istanbul Bilgi University, Istanbul, Turkey
 - 60: Also at Yildiz Technical University, Istanbul, Turkey
 - 61: Also at Hacettepe University, Ankara, Turkey
 - 62: Also at Rutherford Appleton Laboratory, Didcot, United Kingdom
 - 63: Also at School of Physics and Astronomy, University of Southampton, Southampton, United Kingdom
 - 64: Also at Instituto de Astrofísica de Canarias, La Laguna, Spain
 - 65: Also at Utah Valley University, Orem, USA
 - 66: Also at University of Belgrade, Faculty of Physics and Vinca Institute of Nuclear Sciences, Belgrade, Serbia
 - 67: Also at Facoltà Ingegneria, Università di Roma, Roma, Italy
 - 68: Also at Argonne National Laboratory, Argonne, USA
 - 69: Also at Erzincan University, Erzincan, Turkey
 - 70: Also at Mimar Sinan University, Istanbul, Istanbul, Turkey
 - 71: Also at Texas A&M University at Qatar, Doha, Qatar
 - 72: Also at Kyungpook National University, Daegu, Korea
 - 73: Also at University of Visva-Bharati, Santiniketan, India